

Calculation of Derivative Thermodynamic Hydration and Aqueous Partial Molar Properties of Ions Based on Atomistic Simulations

Björn Dahlgren,[†] Maria M. Reif,[‡] Philippe H. Hünenberger,[†] and Niels Hansen^{*,†}

[†]Laboratory of Physical Chemistry, ETH Zürich, Zürich, Switzerland

[‡]Institute for Molecular Modeling and Simulation, University of Natural Resources and Life Sciences, Vienna, Austria

Supporting Information

ABSTRACT: The raw ionic solvation free energies calculated on the basis of atomistic (explicit-solvent) simulations are extremely sensitive to the boundary conditions and treatment of electrostatic interactions used during these simulations. However, as shown recently [Kastenholz, M. A.; Hünenberger, P. H. *J. Chem. Phys.* **2006**, *124*, 224501 and Reif, M. M.; Hünenberger, P. H. *J. Chem. Phys.* **2011**, *134*, 144104], the application of an appropriate correction scheme allows for a conversion of the methodology-dependent raw data into methodology-independent results. In this work, methodology-independent derivative thermodynamic hydration and aqueous partial molar properties are calculated for the Na⁺ and Cl[−] ions at $P^\circ = 1$ bar and $T^- = 298.15$ K, based on the SPC water model and on ion–solvent Lennard-Jones interaction coefficients previously reoptimized against experimental hydration free energies. The hydration parameters considered are the hydration free energy and enthalpy. The aqueous partial molar parameters considered are the partial molar entropy, volume, heat capacity, volume-compressibility, and volume-expansivity. Two alternative calculation methods are employed to access these properties. Method I relies on the difference in average volume and energy between two aqueous systems involving the same number of water molecules, either in the absence or in the presence of the ion, along with variations of these differences corresponding to finite pressure or/and temperature changes. Method II relies on the calculation of the hydration free energy of the ion, along with variations of this free energy corresponding to finite pressure or/and temperature changes. Both methods are used considering two distinct variants in the application of the correction scheme. In variant A, the raw values from the simulations are corrected after the application of finite difference in pressure or/and temperature, based on correction terms specifically designed for derivative parameters at P° and T^- . In variant B, these raw values are corrected prior to differentiation, based on corresponding correction terms appropriate for the different simulation pressures P and temperatures T . The results corresponding to the different calculation schemes show that, except for the hydration free energy itself, accurate methodological independence and quantitative agreement with even the most reliable experimental parameters (ion–pair properties) are not yet reached. Nevertheless, approximate internal consistency and qualitative agreement with experimental results can be achieved, but only when an appropriate correction scheme is applied, along with a careful consideration of standard-state issues. In this sense, the main merit of the present study is to set a clear framework for these types of calculations and to point toward directions for future improvements, with the ultimate goal of reaching a consistent and quantitative description of single-ion hydration thermodynamics in molecular dynamics simulations.

1. INTRODUCTION

The microscopic size of the systems considered and the approximate treatment of electrostatic interactions currently represent two of the most severe limitations in the accuracy of atomistic (explicit-solvent) simulations concerning (bio)-molecular systems in the condensed phase.^{1,2} The problem is particularly severe in the context of systems involving species or functional groups with net charges, e.g., in simulations of protein or electrolyte solutions, and even more so when processes are considered that involve a change in the net charge of a system, e.g., in calculations of solvation free energies for ionic species. Since the earliest calculations of ionic solvation free energies in the 1980s,^{3–6} it has been realized that the raw results can be dramatically sensitive to the boundary conditions and treatment of electrostatic interactions used during these simulations, with typical variations on the order of 100 kJ mol^{−1} or larger for monovalent ions in water.

Recently, however, progress has been made toward the reliable calculation of single-ion solvation properties, by

correcting the raw methodology-dependent simulation results *ex post*, so that methodology-independent values are obtained.^{7–11} The corrected results are then exclusively characteristic of the underlying molecular model, as determined by the representation of the solvent, of the ion, and of the ion–solvent van der Waals interactions, and no longer depend on arbitrary simulation parameters such as the system size or the electrostatic cutoff distance. These values correspond to the idealized situation of an infinite bulk phase exempt of surface polarization, in which electrostatic interactions are exactly Coulombic. Using this correction scheme, a reparametrization of the ion–solvent Lennard-Jones interaction coefficients for Na⁺ and Cl[−] (among other ions) with the SPC water model¹² (as well as the SPC/E model¹³) against experimental hydration

Special Issue: Wilfred F. van Gunsteren Festschrift

Received: March 30, 2012

Published: June 17, 2012

free energies was conducted by Reif and Hünenberger.¹⁰ Three different parameter sets (L, M, and H) were calibrated, corresponding to different assumed values for the absolute intrinsic hydration free energy $\Delta G_{\text{hyd}}^{\ominus}[\text{H}^+]$ of the proton at $P^{\circ} = 1$ bar and $T^{\circ} = 298.15$ K, which is an experimentally elusive quantity.¹¹ An initial assessment of the reoptimized parameters based on experimental quantities other than hydration free energies,¹⁰ including first peak positions in the ion–water radial distribution functions, aqueous salt partial molar volumes, and salt crystal properties, led to preliminary evidence for the appropriateness of set L, calibrated on the basis of $\Delta G_{\text{hyd}}^{\ominus}[\text{H}^+] = -1100$ kJ mol⁻¹. This value is also the one recommended in ref 11 on the basis of a careful analysis of the nearly 100 estimates reported to date for this quantity, relying on various types of experiments and associated extra-thermodynamic assumptions.

The aim of the present study is to investigate the feasibility of calculating and correcting derivative thermodynamic hydration and aqueous partial molar properties for Na⁺ and Cl⁻ at P° and T° , so as to use these quantities as additional validation data for set L with the SPC water model, and for the associated $\Delta G_{\text{hyd}}^{\ominus}[\text{H}^+]$ estimate of -1100 kJ mol⁻¹. More specifically, the hydration parameters considered are the hydration free energy $\Delta G_{\text{hyd}}^{\ominus}$ and enthalpy $\Delta H_{\text{hyd}}^{\ominus}$, and the aqueous partial molar parameters considered are the partial molar entropy s_{aq}^{\ominus} , volume v_{aq}^{\ominus} , isobaric heat capacity $c_{p,\text{aq}}^{\ominus}$, isothermal volume-compressibility $k_{T,\text{aq}}^{\ominus}$, and isobaric volume-expansivity $\alpha_{p,\text{aq}}^{\ominus}$. These quantities are directly connected to the hydration free energy $\Delta G_{\text{hyd}}^{\ominus}$ of the ion, along with its first and second pressure or/and temperature derivatives. For the aqueous partial molar parameters, the connection also involves the corresponding gas-phase molar parameters, which are known analytically for the alkali and halide ions at room temperature. Because these gas-phase parameters permit a trivial interconversion between hydration and aqueous partial molar properties, the hydration parameters $\Delta S_{\text{hyd}}^{\ominus}$, $\Delta V_{\text{hyd}}^{\ominus}$, $\Delta C_{p,\text{hyd}}^{\ominus}$, $\Delta K_{T,\text{hyd}}^{\ominus}$, and $\Delta \alpha_{p,\text{hyd}}^{\ominus}$ are not discussed explicitly here. In contrast, the free energy and enthalpy cannot be formulated in terms of corresponding aqueous partial molar parameters in the absence of a fixed zero point for the energy and are therefore discussed in the form of $\Delta G_{\text{hyd}}^{\ominus}$ and $\Delta H_{\text{hyd}}^{\ominus}$. An alternative, not used in the present work, would be to consider the formation parameters of the aqueous ions instead.

The connection existing between the seven thermodynamic parameters considered here and the hydration free energy $\Delta G_{\text{hyd}}^{\ominus}$, along with its first and second pressure or/and temperature derivatives, suggests one possible approach for the calculation of these properties based on atomistic simulations, *via* finite-difference analysis of $\Delta G_{\text{hyd}}(P, T)$ values calculated at different pressures P and temperatures T . Alternatively, the hydration enthalpy $\Delta H_{\text{hyd}}^{\ominus}$ and the partial molar volume v_{aq}^{\ominus} can also be directly connected to the variations of the energy and volume, respectively, upon inserting the ion into a pure-liquid sample of infinite extent. If the pressure and temperature dependences of these variations are known, this second connection applies to five of the thermodynamic parameters considered here, i.e., all except $\Delta G_{\text{hyd}}^{\ominus}$ and s_{aq}^{\ominus} . This suggests another possible approach for the calculation of these five properties based on atomistic simulations, *via* finite-difference analysis of $\Delta H_{\text{hyd}}(P, T)$ and $v_{\text{aq}}(P, T)$ values calculated from the above energy and volume differences at different pressures P and temperatures T .

The two strategies outlined above for calculating (a subset of) the seven properties of interest are both considered and

compared in the present study. The approach relying on energy and volume differences between aqueous systems excluding or including the ion, referred to here as method I, is in principle simpler because it only requires two simulations per P, T -point. The approach relying on the hydration free energy, referred to here as method II, is somewhat more complicated because it requires a calculation of the reversible work associated with the cavitation and charging processes, i.e., multiple simulations at each P, T -point.

Additionally, for each of these two methods, two distinct variants are considered for the application of the correction scheme⁹ to the raw simulation results (energy and volume differences in method I, hydration free energies in method II). In variant A, the raw values are corrected after application of finite difference in pressure or/and temperature, based on correction terms specifically designed for derivative thermodynamic parameters at P° and T° . In variant B, these raw values are corrected prior to differentiation, based on corresponding correction terms appropriate for the different simulation pressures P and temperatures T . The four combinations of methods and variants are thus IA, IB, IIA, and IIB. For a given molecular model, these different schemes become entirely equivalent in the limit of infinitesimal finite-difference intervals and infinite sampling times. However, the corresponding results may differ in practice due to finite-difference errors and finite simulation times, and the observed discrepancies, along with the consideration of different system sizes, are expected to provide an indication on the level of precision and convergence of the calculated numbers.

It should be stressed that the calculation of derivative thermodynamic properties and their use as validation data for a given molecular model in the context of ionic solvation, although of very fundamental significance, is a highly nontrivial task. The main issues affecting these types of calculation are the following:

1. Long simulation times are required to reach estimates that are both precise and converged. This requirement results from a trade-off between the size of the finite-difference interval and the sampling time of the two compared simulations. On the one hand, the precision of a fully converged finite-difference estimate decreases with increasing size of the interval considered, due to the increasing contribution of nonlinear components. On the other hand, the error on the calculated number at finite simulation time decreases with increasing interval size, because it depends on the statistical uncertainties affecting the two compared values, divided by this interval size. As a result, precise estimates, implying a reasonably small finite-difference interval, can only be calculated to an acceptable level of convergence using relatively long simulations.
2. The simplified force-field representation is typically less adequate and accurate when considering derivative as opposed to nonderivative thermodynamic properties. This limitation results from the more limited emphasis generally placed on the reproduction of derivative properties during force-field design and parametrization. In general, the functional form and parameters of a force field are selected primarily to reproduce observables related to free energies, enthalpies, and volumes, e.g., the density, enthalpy of vaporization, and excess free energy for a liquid,^{14,15} or the solvation free energy for an ion.¹⁰

Their accuracies in terms of derivative properties, such as the entropy, heat capacity, compressibility, and expansivity, are usually lower, due to both a limited functional flexibility and a lower weight attributed to these properties in the parametrization procedure.

3. The correction scheme for single-ion solvation free energies,⁸ recently generalized to derivative thermodynamic properties,⁹ is affected by errors concerning its input parameters. This generalized scheme requires experimental estimates for the pressure and temperature dependences of the effective ionic radius R_b , of the solvent density ρ , dielectric permittivity ϵ , air–liquid interfacial potential χ , and derivative of this potential with respect to the inverse curvature radius for convex $\tilde{\chi}_+$ or concave $\tilde{\chi}_-$ interfaces, as well as corresponding estimates ρ' , ϵ' , χ' , $\tilde{\chi}'_+$, and $\tilde{\chi}'_-$, respectively, for the solvent model employed in the simulations. Ambiguities and uncertainties in the definition of these functions result in corresponding errors on the corrected values.
4. The experimental data to compare with is ambiguous. Similarly to the proton hydration free energy $\Delta G_{\text{hyd}}^\ominus[\text{H}^+]$ (see above), the derivative thermodynamic hydration and aqueous partial molar parameters of this species are experimentally elusive.¹¹ Although values have been suggested for $\Delta H_{\text{hyd}}^\ominus[\text{H}^+]$, $s_{\text{aq}}^\ominus[\text{H}^+]$, $v_{\text{aq}}^\ominus[\text{H}^+]$, $c_{p,\text{aq}}^\ominus[\text{H}^+]$, $k_{T,\text{aq}}^\ominus[\text{H}^+]$, and $a_{p,\text{aq}}^\ominus[\text{H}^+]$, see, e.g., the recommended values in ref 11, they should be taken with great caution in view of the sparseness and indirect nature of the corresponding experimental determinations, and of their dependence on specific extra-thermodynamic assumptions. As a result, comparison of data on the basis of salt parameters (e.g., $\text{Na}^+ + \text{Cl}^-$) or of parameter differences between ions of identical charges (e.g., Na^+ vs K^+) is certainly at present more meaningful than single-ion comparisons. For the second-derivative quantities c_p^\ominus , k_T^\ominus , and a_p^\ominus , however, the experimental estimates even for these sums or differences are not highly reliable, in view of the very small number of independent determinations and of the limited consistency among the resulting estimates.¹¹

In view of these difficulties, the goal of the present study is to cut a first path through an unexplored jungle rather than to reach quantitative agreement with sometimes highly uncertain experimental data. Note, finally, that if many previous simulation studies have investigated ionic solvation free energies $\Delta G_{\text{hyd}}^\ominus$ and (approximate) enthalpies $\Delta H_{\text{hyd}}^\ominus$ (see refs 10 and 11, and references therein), only a few have considered ionic solvation entropies^{16–21} $\Delta S_{\text{hyd}}^\ominus$ and aqueous ion partial molar volumes^{9,22–24} v_{aq}^\ominus , while none to our knowledge has considered the derivative properties $c_{p,\text{aq}}^\ominus$, $k_{T,\text{aq}}^\ominus$, and $a_{p,\text{aq}}^\ominus$.

2. THEORY

2.1. Derivative Thermodynamic Parameters. The thermodynamic parameters considered here are the Gibbs free energy G , enthalpy H , entropy S , volume V , isobaric heat capacity C_p , isothermal volume-compressibility K_T , and isobaric volume-expansivity A_p . Collectively denoting these seven variables as Y , they are related to the free energy by

$$Y = \hat{O}_Y G \quad (1)$$

where \hat{O}_Y is the thermodynamic-derivative operator¹¹ associated with the parameter Y . These operators are given by

$$\begin{aligned} \hat{O}_G &= 1 \\ \hat{O}_H &= 1 - T\partial_T [= -T^2\partial_T T^{-1}] & \hat{O}_V &= \partial_p \\ \hat{O}_S &= -\partial_T & \hat{O}_{K_T} &= -\partial_p^2 \\ \hat{O}_{C_p} &= -T\partial_T^2 [= \partial_T(1 - T\partial_T)] & \hat{O}_{A_p} &= \partial_{p,T}^2 \end{aligned} \quad (2)$$

where ∂_p and ∂_T represent partial differentiation with respect to pressure or temperature, respectively, the other variable as well as the system composition being kept constant, and ∂^2 indicates corresponding second (self or cross) derivatives. Main and alternative operator expressions are provided for H and C_p , the alternative ones between square brackets. For H , the two expressions are related to the Gibbs and Gibbs–Helmholtz equations, respectively. For C_p , they correspond to the temperature derivative of the entropy and enthalpy, respectively. The two pairs of expressions are equivalent in the context of exact derivatives, but may differ numerically when translated into corresponding finite-difference equations. Unless otherwise specified, the main expressions are used in the present work for both H and C_p . The extensive variables K_T and A_p are referred to as the volume-compressibility and the volume-expansivity, respectively. These names are selected to distinguish K_T and A_p from the intensive compressibility κ_T and expansivity (thermal expansion coefficient) α_p , respectively, the definition of which is ambiguous in the context of partial molar properties.⁹

For a pure gas-phase species, the molar parameter corresponding to variable Y will be noted as y_g , where $y = \mu, h, s, v, c_p, k_T$, or a_p for $Y = G, H, S, V, C_p, K_T$, or A_p . For a single solute species in aqueous solution, the corresponding partial molar parameters will be noted as y_{aq} . The hydration parameters of the species are then defined by

$$\Delta Y_{\text{hyd}} = y_{\text{aq}} - y_g \quad (3)$$

Obviously, eq 1 also applies to gas-phase molar and aqueous partial molar properties, as well as to hydration parameters, i.e.

$$y_g = \hat{O}_Y \mu_g, y_{\text{aq}} = \hat{O}_Y \mu_{\text{aq}} \text{ and } \Delta Y_{\text{hyd}} = \hat{O}_Y \Delta G_{\text{hyd}} \quad (4)$$

Note that all of the thermodynamic parameters considered in this work are intrinsic (as opposed to real), i.e., they exclude any contribution associated with the crossing of the polarized air–water interface.¹¹

2.2. Standard States. Most commonly, although by no means systematically, experimental thermodynamic data pertaining to ionic solvation are tabulated in the literature according to the *bbme_T* standard-state convention.¹¹ In this case, reference is made to the standard pressure $P^\circ = 1$ bar, molality $b^\circ = 1$ mol kg^{−1}, and temperature $T^- = 298.15$ K. Since formation parameters are not considered in the present work, the definition of a standard state for the electron (ideal electron gas at temperature T^- with properties calculated according to Fermi–Dirac statistics in *bbme_T*) is irrelevant here.

In the *bbme_T* convention, the standard gas-phase molar properties of a species, noted here as y_g^\ominus , refer to a pure ideal gas (no intermolecular interactions) at pressure P° and temperature T^- . Note in particular that the ideal-gas law implies

$$v_g^\ominus = (P^\circ)^{-1}RT^-, k_{T,g}^\ominus = (P^\circ)^{-2}RT^- \text{ and } a_{p,g}^\ominus = (P^\circ)^{-1}R \quad (5)$$

where R is the ideal gas constant. For closed-shell monoatomic species exempt of thermally accessible electronically excited states at T^- , as is the case for, e.g., alkali cations and halide anions at room temperature,¹¹ the Sackur–Tetrode equation^{25–27} implies in addition

$$s_g^\ominus = R\{(5/2) + \ln[CM^{3/2}(P^\ominus)^{-1}(T^-)^{5/2}]\} \text{ and} \\ c_{p,g}^\ominus = (5/2)R \text{ for, e.g., } Na^+, Cl^- \quad (6)$$

where M is the molar mass of the species and

$$C = \frac{(2\pi)^{3/2} R^{5/2}}{N_A^4 h^3} = 820.512 \text{ (kg mol}^{-1}\text{)}^{-3/2} \text{ bar K}^{-5/2} \quad (7)$$

N_A being the Avogadro constant and h the Planck constant. Note that eq 6 is in principle not applicable to the proton and the electron, where Fermi–Dirac statistics should be used instead of Boltzmann statistics.^{11,28} Although the resulting values differ noticeably for the electron, eq 6 still provides an excellent approximation in the case of the proton. In the *bbme_T* convention, the standard aqueous partial molar properties of a species, noted here as y_{aq}^\ominus , refer to the solute alone in an ideal aqueous solution (no direct or solvent-mediated solute–solute interactions) at pressure P^\ominus , molality b^\ominus , and temperature T^- .

The direct outcome of theoretical calculations, e.g., based on atomistic simulations, generally concerns fixed-point rather than standard parameters.¹¹ The fixed-point gas-phase molar properties of a species, noted here as y_g^\square , refer to the translationally motionless species at temperature T^- , surrounded by vacuum. In contrast to the corresponding standard parameters y_g^\ominus , these parameters no longer depend on the choice of a standard pressure P^\ominus . The removal of molecular translation implies in particular that in terms of fixed-point quantities, the molar volume as well as its derivatives vanish, i.e.

$$v_g^\square = 0, k_{T,g}^\square = 0, \text{ and } a_{p,g}^\square = 0 \quad (8)$$

For closed-shell monoatomic species exempt of thermally accessible electronically excited states at T^- , as is the case for, e.g., alkali cations and halide anions at room temperature, one also has

$$s_g^\square = 0 \text{ and } c_{p,g}^\square = 0 \text{ for, e.g., } Na^+, Cl^- \quad (9)$$

The fixed-point aqueous partial molar properties of a species, noted here as y_{aq}^\square , refer to the translationally motionless solute species at temperature T^- , surrounded by pure water at pressure P^\ominus and temperature T^- . In contrast to the corresponding standard parameters y_{aq}^\ominus , these parameters only depend on the choice of a standard pressure P^\ominus via its effect on the state of the solvent, and no longer rely on the definition of a standard molality b^\ominus .

Considering either fixed-point or standard quantities, eq 3 provides a definition for the corresponding hydration parameters, referred to as point-to-point or standard, respectively, i.e.

$$\Delta Y_{hyd}^\square = y_{aq}^\square - y_g^\square \quad (10)$$

and

$$\Delta Y_{hyd}^\ominus = y_{aq}^\ominus - y_g^\ominus \quad (11)$$

Note in particular that the symbols ΔY_{hyd}^\square and y_{aq}^\square can be used interchangeably for $Y = V, K_T$, and A_p (due to eq 8), as well as for S and C_p in the context of alkali and halide ions (due to eq 9). Point-to-point hydration parameters can also be viewed as resulting from an alternative standard-state convention where identical effective solute concentrations (molarities) are selected for the gas-phase and aqueous states. Such a convention is also commonly used in the literature concerning ionic thermodynamics.^{29–36}

In terms of fixed-point gas-phase molar and aqueous partial molar properties, as well as point-to-point hydration parameters, eq 4 becomes

$$y_g^\square = \hat{O}_Y \mu_g^\square, y_{aq}^\square = \hat{O}_Y \mu_{aq}^\square, \text{ and } \Delta Y_{hyd}^\square = \hat{O}_Y \Delta G_{hyd}^\square \quad (12)$$

with the convention that \hat{O}_Y applied to a function of P^\ominus and T^- implies differentiation of the corresponding P, T -dependent quantity followed by evaluation at P^\ominus and T^- . In terms of standard gas-phase molar properties, eq 4 also implies

$$y_g^\ominus = \hat{O}_Y \mu_g^\ominus \quad (13)$$

However, corresponding equations for standard aqueous partial molar and hydration parameters must be considered more carefully, due to the presence of an ambiguity concerning the derivatives of the solvent density (see below).

The difference between fixed-point and standard quantities is related to the phase-space volume accessible to the species in terms of translational degrees of freedom in its standard state.¹¹ The translational momentum-space volume is identical in the gas-phase and aqueous states, and proportional to $(MT^-)^{3/2}$. However, the translational coordinate-space volume differs between the two states. For gas-phase species, this coordinate-space volume is the ideal-gas molar volume $(P^\ominus)^{-1}RT^-$, as determined by P^\ominus and T^- . In this case, the fixed-point molar properties can be standardized as

$$y_g^\ominus = y_g^\square + \Delta y_{g \rightarrow \ominus}^\square \\ = y_g^\square - R\hat{O}_Y \left\{ T^- \ln \left[\tilde{C} (MT^-)^{3/2} \frac{RT^-}{P^\ominus} \right] \right\} \quad (14)$$

where $\tilde{C} = R^{-1}C$. It is easily verified that eqs 5 and 8, as well as eqs 6 and 9 in the specific case of alkali and halide ions, satisfy the connection of eq 14. For aqueous species, the coordinate-space volume is the effective molar volume $(b^\ominus \rho^\ominus)^{-1}$ accessible to the solute species, as determined by b^\ominus and ρ^\ominus , where ρ^\ominus is the pure-solvent density at P^\ominus and T^- . In this case, the fixed-point partial molar properties can be standardized as

$$y_{aq}^\ominus = y_{aq}^\square + \Delta y_{aq \rightarrow \ominus}^\square \\ = y_{aq}^\square - R\hat{O}_Y \left\{ T^- \ln \left[\tilde{C} (MT^-)^{3/2} \frac{1}{b^\ominus \rho^\ominus} \right] \right\} \quad (15)$$

Given the definitions of eqs 10 and 11, it follows from eqs 14 and 15 that the two types of hydration parameters are connected by

$$\Delta Y_{hyd}^\ominus = \Delta Y_{hyd}^\square + \Delta \Delta Y_{hyd \rightarrow \ominus}^\square \\ = \Delta Y_{hyd}^\square + R\hat{O}_Y \left\{ T^- \ln \left[\frac{RT^- b^\ominus \rho^\ominus}{P^\ominus} \right] \right\} \quad (16)$$

Finally, in analogy with eq 12 for fixed-point parameters, eq 13 for the standard gas-phase properties can be complemented by

$$y_{\text{aq}}^{\ominus} = \hat{O}_Y \mu_{\text{aq}}^{\ominus} \text{ and } \Delta Y_{\text{hyd}}^{\ominus} = \hat{O}_Y \Delta G_{\text{hyd}}^{\ominus} \quad (17)$$

for the standard aqueous partial molar and hydration properties, respectively.

The strict application of eqs 15 and 16 implies that the operator \hat{O}_Y acting on ρ^{\ominus} introduces corresponding derivatives into the resulting expressions for standard derivative thermodynamic properties. This choice represents the so-called standard variant of the solute standard-state definition.^{9,11} Adopting this convention leads to a number of counterintuitive results, which are most easily illustrated by considering the hypothetical case of a noninteracting and volume-free single-particle “ghost” solute. For such a species, all fixed-point and point-to-point parameters evaluate to zero. However, eqs 15 and 16 imply, for example, that the particle has a standard hydration enthalpy $\Delta H_{\text{hyd}}^{\ominus}$ differing from the mere $-RT^-$ term, although it presents no interaction with the solvent, and that it has a nonvanishing standard aqueous partial molar volume v_{aq}^{\ominus} (as well as derivatives $k_{T,\text{aq}}^{\ominus}$ and $a_{p,\text{aq}}^{\ominus}$), although it has been assumed volume-free. The corresponding partial molar entropy s_{aq}^{\ominus} also differs from that expected for a free particle within an effective molar volume $(b^{\ominus}\rho^{\ominus})^{-1}$, while the corresponding partial molar heat capacity $c_{p,\text{aq}}^{\ominus}$ differs from the expected value of $(3/2)R$. Furthermore, the values of these unexpected additional contributions are related to the expansivity and compressibility of pure water, two properties that appear to be entirely irrelevant in terms of hydration under isobaric and isothermal conditions. Their occurrence is even more surprising considering that the particle does not “feel” the solvent and should thus be insensitive to its nature beyond the role of ρ^{\ominus} in determining the effective molar volume associated with the solute standard state.

These counterintuitive features can be alleviated by introducing a slightly different definition for the solute standard state, referred to as the density-corrected variant,^{9,11} in which the derivatives of ρ^{\ominus} are omitted in the application of \hat{O}_Y . The standard parameters in this density-corrected variant will be noted with a star superscript, to distinguish them from the corresponding quantities in the standard variant. The two variants are equivalent in terms of all standard gas-phase molar parameters, of the standard chemical potential in the aqueous phase, and of the hydration free energy, i.e.

$$y_{\text{g}}^{\ominus*} = y_{\text{g}}^{\ominus}, \mu_{\text{aq}}^{\ominus*} = \mu_{\text{aq}}^{\ominus}, \text{ and } \Delta G_{\text{hyd}}^{\ominus*} = \Delta G_{\text{hyd}}^{\ominus} \quad (18)$$

However, they differ in terms of the derivative hydration parameters and aqueous partial molar properties, namely, $\Delta H_{\text{hyd}}^{\ominus*}$, $s_{\text{aq}}^{\ominus*}$, $v_{\text{aq}}^{\ominus*}$, $c_{p,\text{aq}}^{\ominus*}$, $k_{T,\text{aq}}^{\ominus*}$ and $a_{p,\text{aq}}^{\ominus*}$ in the density-corrected variant vs $\Delta H_{\text{hyd}}^{\ominus}$, s_{aq}^{\ominus} , v_{aq}^{\ominus} , $c_{p,\text{aq}}^{\ominus}$, $k_{T,\text{aq}}^{\ominus}$ and $a_{p,\text{aq}}^{\ominus}$ in the standard one.

In the density-corrected variant, eq 14 is unaltered, i.e.

$$y_{\text{g}}^{\ominus*} = y_{\text{g}}^{\square} + \Delta y_{\text{g}}^{\square \rightarrow \ominus*} = y_{\text{g}}^{\square} + \Delta y_{\text{g}}^{\square \rightarrow \ominus} \quad (19)$$

while eq 15 is modified to

$$y_{\text{aq}}^{\ominus*} = y_{\text{aq}}^{\square} + \Delta y_{\text{aq}}^{\square \rightarrow \ominus*} \\ = y_{\text{aq}}^{\square} - R\hat{O}_Y \left\{ T^- \ln \left[\tilde{C}(MT^-)^{3/2} \frac{1}{b^{\ominus}\rho^*} \right] \right\} \quad (20)$$

where ρ^* is a strict constant (no derivatives upon application of \hat{O}_Y), the value of which is set to the pure-solvent density at P^{\ominus} and T^- , i.e.

$$\rho^* = \rho^{\ominus} \quad (21)$$

Accordingly, with the definition of eq 11 translated to

$$\Delta Y_{\text{hyd}}^{\ominus*} = y_{\text{aq}}^{\ominus*} - y_{\text{g}}^{\ominus*} = y_{\text{aq}}^{\ominus*} - y_{\text{g}}^{\ominus} \quad (22)$$

Equation 16 is modified to

$$\Delta Y_{\text{hyd}}^{\ominus*} = \Delta Y_{\text{hyd}}^{\square} + \Delta \Delta Y_{\text{hyd}}^{\square \rightarrow \ominus*} \\ = \Delta Y_{\text{hyd}}^{\square} + R\hat{O}_Y \left\{ T^- \ln \left[\frac{RT^- b^{\ominus} \rho^*}{P^{\ominus}} \right] \right\} \quad (23)$$

Adopting this alternative convention alleviates the counterintuitive observations described above in the illustrative context of a single-particle “ghost” solute. In the density-corrected variant, eqs 20 and 23 imply, for example, that the particle has a standard hydration enthalpy $\Delta H_{\text{hyd}}^{\ominus*}$ exactly equal to $-RT^-$ and that it has a vanishing standard aqueous partial molar volume $v_{\text{aq}}^{\ominus*}$ (as well as derivatives $k_{T,\text{aq}}^{\ominus*}$ and $a_{p,\text{aq}}^{\ominus*}$). The corresponding partial molar entropy $s_{\text{aq}}^{\ominus*}$ is also the one expected for a free particle within an effective molar volume $(b^{\ominus}\rho^{\ominus})^{-1}$, and the corresponding partial molar heat capacity $c_{p,\text{aq}}^{\ominus*}$ evaluates to $(3/2)R$ as expected. Furthermore, the standard properties in the density-corrected variant no longer depend on the expansivity and compressibility of the pure solvent. These observations are much more intuitive compared to those made in the context of the standard variant. However, they come at the cost of giving up the direct relationship between free energy and derivative thermodynamic properties *via* the thermodynamic-derivative operators of eq 2, i.e., in the density-corrected variant, eq 13 can no longer be complemented by equations of the form of eq 17.

As explained in ref 11, the reason for distinguishing the two above solute standard-state variants is that different types of experiments probing derivative thermodynamic properties may lead, as their natural outcome, to standardized results corresponding to either of the two variants, both simply reported as “standard” in the literature. The differences between quantities reported in the two variants are then given by

$$\Delta y_{\text{g}}^{\ominus* \rightarrow \ominus} = \Delta y_{\text{g}}^{\square \rightarrow \ominus} - \Delta y_{\text{g}}^{\square \rightarrow \ominus*} = 0 \quad (24)$$

$$\Delta y_{\text{aq}}^{\ominus* \rightarrow \ominus} = \Delta y_{\text{aq}}^{\square \rightarrow \ominus} - \Delta y_{\text{aq}}^{\square \rightarrow \ominus*} = R\hat{O}_Y \left\{ T^- \ln \left[\frac{\rho^{\ominus}}{\rho^*} \right] \right\} \quad (25)$$

and

$$\Delta \Delta Y_{\text{hyd}}^{\ominus* \rightarrow \ominus} = \Delta \Delta Y_{\text{hyd}}^{\square \rightarrow \ominus} - \Delta \Delta Y_{\text{hyd}}^{\square \rightarrow \ominus*} \\ = R\hat{O}_Y \left\{ T^- \ln \left[\frac{\rho^{\ominus}}{\rho^*} \right] \right\} \quad (26)$$

This ambiguity may represent a non-negligible source of error, especially for aqueous partial molar volumes, heat capacities, and compressibilities. For example, for the Na^+ and Cl^- ions, v_{aq}^{\square} , $c_{p,\text{aq}}^{\square}$ and $k_{T,\text{aq}}^{\square}$ are in magnitude on the order of $10^{-5} \text{ m}^3 \text{ mol}^{-1}$, $10^2 \text{ J mol}^{-1} \text{ K}^{-1}$, and $10^{-9} \text{ m}^3 \text{ mol}^{-1} \text{ bar}^{-1}$, respectively (section 4), to be compared with $\Delta v_{\text{aq}}^{\ominus \rightarrow \ominus*}$, $\Delta c_{p,\text{aq}}^{\ominus \rightarrow \ominus*}$, and

Table 1. Constants Required for Standard-State Interconversions of Thermodynamic Properties^a

y_g	unit	$\Delta y_g^{\square \rightarrow \odot*}$		$\Delta y_g^{\odot* \rightarrow \odot}$	
		equation ^b	numerical value ^c	equation ^d	numerical value
μ_g	[kJ mol ⁻¹]	$-RT^- \ln[CM^{3/2}(P^\circ)^{-1}(T^-)^{5/2}]$	$-51.94 - 3.72 f_M$	0	0
h_g	[kJ mol ⁻¹]	$(5/2)RT^-$	6.20	0	0
s_g	[J mol ⁻¹ K ⁻¹]	$R\{(5/2) + \ln[CM^{3/2}(P^\circ)^{-1}(T^-)^{5/2}]\}$	$195.01 + 12.47 f_M$	0	0
v_g	[m ³ mol ⁻¹]	$(P^\circ)^{-1}RT^-$	2.48×10^{-2}	0	0
$c_{p,g}$	[J mol ⁻¹ K ⁻¹]	$(5/2)R$	20.79	0	0
$k_{T,g}$	[m ³ mol ⁻¹ bar ⁻¹]	$(P^\circ)^{-2}RT^-$	2.48×10^{-2}	0	0
$a_{p,g}$	[m ³ mol ⁻¹ K ⁻¹]	$(P^\circ)^{-1}R$	8.31×10^{-5}	0	0
y_{aq}	unit	$\Delta y_{aq}^{\square \rightarrow \odot*}$		$\Delta y_{aq}^{\odot* \rightarrow \odot}$	
		equation ^e	numerical value ^{c,f}	equation ^{g,h}	numerical value ⁱ
μ_{aq}	[kJ mol ⁻¹]	$-RT^- \ln[C(MT^-)^{3/2}(Rb^\circ \rho^*)^{-1}]$	$-43.99 - 3.72 f_M$	0	0
h_{aq}	[kJ mol ⁻¹]	$(3/2)RT^-$	3.72	$-R(T^-)^2 \partial_T \ln \rho^\odot$	0.19
s_{aq}	[J mol ⁻¹ K ⁻¹]	$R\{(3/2) + \ln[C(MT^-)^{3/2}(Rb^\circ \rho^*)^{-1}]\}$	$160.02 + 12.47 f_M$	$-RT^- \partial_T \ln \rho^\odot$	0.64
v_{aq}	[m ³ mol ⁻¹]	0	0	$RT^- \partial_p \ln \rho^\odot$	1.12×10^{-6}
$c_{p,aq}$	[J mol ⁻¹ K ⁻¹]	$(3/2)R$	12.47	$-RT^- \{2\partial_T \ln \rho^\odot + T^- \partial_T^2 \ln \rho^\odot\}$	8.39
$k_{T,aq}$	[m ³ mol ⁻¹ bar ⁻¹]	0	0	$-RT^- \partial_p^2 \ln \rho^\odot$	2.88×10^{-10}
$a_{p,aq}$	[m ³ mol ⁻¹ K ⁻¹]	0	0	$R\partial_p \ln \rho^\odot + RT^- \partial_{p,T}^2 \ln \rho^\odot$	9.92×10^{-10}
ΔY_{hyd}	unit	$\Delta \Delta Y_{hyd}^{\square \rightarrow \odot*}$		$\Delta \Delta Y_{hyd}^{\odot* \rightarrow \odot}$	
		equation ^j	numerical value ^f	equation ^{h,k}	numerical value ⁱ
ΔG_{hyd}	[kJ mol ⁻¹]	$RT^- \ln[(P^\circ)^{-1}RT^- b^\circ \rho^*]$	7.95	0	0
ΔH_{hyd}	[kJ mol ⁻¹]	$-RT^-$	-2.48	$-R(T^-)^2 \partial_T \ln \rho^\odot$	0.19
ΔS_{hyd}	[J mol ⁻¹ K ⁻¹]	$-R\{1 + \ln[(P^\circ)^{-1}RT^- b^\circ \rho^*]\}$	-34.98	$-RT^- \partial_T \ln \rho^\odot$	0.64
ΔV_{hyd}	[m ³ mol ⁻¹]	$-(P^\circ)^{-1}RT^-$	-2.48×10^{-2}	$RT^- \partial_p \ln \rho^\odot$	1.12×10^{-6}
$\Delta C_{p,hyd}$	[J mol ⁻¹ K ⁻¹]	$-R$	-8.31	$-RT^- \{2\partial_T \ln \rho^\odot + T^- \partial_T^2 \ln \rho^\odot\}$	8.39
$\Delta K_{T,hyd}$	[m ³ mol ⁻¹ bar ⁻¹]	$-(P^\circ)^{-2}RT^-$	-2.48×10^{-2}	$-RT^- \partial_p^2 \ln \rho^\odot$	2.88×10^{-10}
$\Delta A_{p,hyd}$	[m ³ mol ⁻¹ K ⁻¹]	$-(P^\circ)^{-1}R$	-8.31×10^{-5}	$R\partial_p \ln \rho^\odot + RT^- \partial_{p,T}^2 \ln \rho^\odot$	9.92×10^{-10}

^aThe reported quantities $\Delta y_g^{\square \rightarrow \odot}$ (eq 14), $\Delta y_g^{\odot* \rightarrow \odot}$ (eq 24), $\Delta y_{aq}^{\square \rightarrow \odot}$ (eq 15), $\Delta y_{aq}^{\odot* \rightarrow \odot}$ (eq 25), $\Delta \Delta Y_{hyd}^{\square \rightarrow \odot}$ (eq 16), and $\Delta \Delta Y_{hyd}^{\odot* \rightarrow \odot}$ (eq 26) permit the interconversion between fixed-point or point-to-point (\square superscript) and standard (\odot superscript) quantities in the standard (no star superscript) and density-corrected (star superscript) variants. Expressions and numerical values are provided for the free energy G , enthalpy H , entropy S , volume V , heat capacity C_p , volume-compressibility K_T , and volume-expansivity A_p . The numerical values refer to the standard pressure $P^\circ = 1$ bar, molality $b^\circ = 1$ mol kg⁻¹, and temperature $T^- = 298.15$ K, and to water as a solvent. ^bEquations 14 and 19 with $\tilde{C} = R^{-1}C$ and C defined by eq 7. ^cThe factor f_M is defined as $f_M = \ln(M/M^\circ)$, where M is the molar mass of the species and $M^\circ = 1$ kg mol⁻¹. ^dEquation 24. ^eEquation 20 with $\tilde{C} = R^{-1}C$, C defined by eq 7, and ρ^* defined by eq 21 as a strict constant equal to ρ^\odot . ^fThe entries for the free energy and entropy are based on ρ^* set to the water density ρ^\odot as reported in Table 3. ^gEquation 25. ^hAlthough $\ln \rho^\odot$ should formally rather be written $\ln[\rho^\odot/\rho^*]$, to avoid a dependence on the arbitrary unit selected for ρ^\odot , this dependence has no influence on the derivatives of the logarithm involved in these expressions. ⁱBased on the water density ρ^\odot , as well as its pressure or/and temperature derivatives $\partial_p \rho^\odot$, $\partial_p^2 \rho^\odot$, $\partial_T \rho^\odot$, $\partial_T^2 \rho^\odot$, and $\partial_{p,T}^2 \rho^\odot$ as reported in Table 3 (the values for the volume-compressibility and volume-expansivity reported in Table IV of ref 9 and Table 4.1 of ref 11 differ slightly due to the use of different $\rho(P,T)$ data for water). ^jEquation 23 with ρ^* defined by eq 21 as a strict constant equal to ρ^\odot . ^kEquation 26.

$\Delta k_{T,aq}^{\odot \rightarrow \odot*}$ evaluating to 1.12×10^{-6} m³ mol⁻¹, 8.39 J mol⁻¹ K⁻¹, and 2.88×10^{-10} m³ mol⁻¹ bar⁻¹, respectively. In the present work, this difficulty is circumvented by assuming experimental data appropriate for the standard variant in the case of the free energy, enthalpy, entropy, and heat capacity, and in the density-corrected variant in the case of the volume, volume-compressibility, and volume-expansivity, converting them to point-to-point (hydration parameters) or fixed-point (aqueous partial molar parameters) values, and performing the comparison between simulation and experimental results in terms of the latter values only. This assumption concerning the actual nature of literature data tabulated as “standard” is motivated by the type of experiments usually performed to evaluate these parameters, as detailed in ref 11 (see pp 171–177 therein).

For convenience, the constants $\Delta y_g^{\square \rightarrow \odot}$ (eq 14), $\Delta y_g^{\odot* \rightarrow \odot}$ (eq 24), $\Delta y_{aq}^{\square \rightarrow \odot}$ (eq 15), $\Delta y_{aq}^{\odot* \rightarrow \odot}$ (eq 25), $\Delta \Delta Y_{hyd}^{\square \rightarrow \odot}$ (eq 16), and $\Delta \Delta Y_{hyd}^{\odot* \rightarrow \odot}$ (eq 26), required for the interconversion between fixed-point and standard quantities in the standard or density-corrected variants, are provided in Table 1. The analytical standard (eqs 5 and 6) and fixed-point (eqs 8 and

9) gas-phase parameters, along with experimental estimates for the corresponding hydration and aqueous partial molar parameters, are reported in Table 2 for the Na⁺ and Cl⁻ ions as well as the proton. Note that the aqueous and hydration parameters reported in this table represent experimentally elusive quantities and are thus to be considered with some caution.¹¹

2.3. Calculation of Derivative Thermodynamic Properties. Two alternative methods can be employed to evaluate derivative single-ion hydration and aqueous partial molar properties based on atomistic simulations, referred to here as methods I and II. In both cases, the outcome of the calculations is raw point-to-point (hydration parameters) or fixed-point (aqueous partial molar parameters) quantities. These must be appropriately corrected for finite-system and approximate-electrostatics errors, as described in section 2.4, where two variants in the application of the correction scheme, referred to as variants A and B, are distinguished. The comparison with experimental results is then performed directly in terms of these corrected point-to-point or fixed-point parameters.

Table 2. Standard and Fixed-Point or Point-to-Point Thermodynamic Parameters for the Na⁺ and Cl[−] Ions As Well As the Proton^a

param. ^b	ion	ΔG [kJ mol ^{−1}]	ΔH [kJ mol ^{−1}]	s [J mol ^{−1} K ^{−1}]	c _p [J mol ^{−1} K ^{−1}]	ν [m ³ mol ^{−1}]	k _T [m ³ mol ^{−1} bar ^{−1}]	a _p [m ³ mol ^{−1} K ^{−1}]
y _g [⊙] = y _g ^{⊙*}	H ⁺	1513.32 ^c	1533.10 ^c	108.95 ^{d,e}	20.79 ^e	2.48 × 10 ^{−2f}	2.48 × 10 ^{−2f}	8.31 × 10 ^{−5f}
	Na ⁺	570.71 ^c	606.31 ^c	147.96 ^{d,e}	20.79 ^e	2.48 × 10 ^{−2f}	2.48 × 10 ^{−2f}	8.31 × 10 ^{−5f}
	Cl [−]	−235.77 ^c	−230.08 ^c	153.36 ^{d,e}	20.79 ^e	2.48 × 10 ^{−2f}	2.48 × 10 ^{−2f}	8.31 × 10 ^{−5f}
y _g [□]	H ⁺	1539.61 ^{d,g}	1526.90 ^g	0 ^h	0 ^h	0 ⁱ	0 ⁱ	0 ⁱ
	Na ⁺	608.63 ^{d,g}	600.11 ^g	0 ^h	0 ^h	0 ⁱ	0 ⁱ	0 ⁱ
	Cl [−]	−196.24 ^{d,g}	−236.28 ^g	0 ^h	0 ^h	0 ⁱ	0 ⁱ	0 ⁱ
y _{aq} [⊙]	H ⁺	413.32 ^j	394.06 ^j	−22.00 ^k	−65.00 ^k	−3.38 × 10 ^{−6l}	17.88 × 10 ^{−10l}	−2.90 × 10 ^{−8l}
	Na ⁺	151.25 ^j	153.82 ^j	37.21 ^k	−22.97 ^k	−4.74 × 10 ^{−6l}	−24.57 × 10 ^{−10l}	2.52 × 10 ^{−8l}
	Cl [−]	−544.37 ^j	−561.17 ^j	77.93 ^k	−61.03 ^k	−23.33 × 10 ^{−6l}	−18.41 × 10 ^{−10l}	4.72 × 10 ^{−8l}
y _{aq} ^{⊙*}	H ⁺	413.32 ^m	393.86 ^m	−22.64 ^m	−73.39 ^m	−4.50 × 10 ^{−6k}	15.00 × 10 ^{−10k}	−3.00 × 10 ^{−8k}
	Na ⁺	151.25 ^m	153.63 ^m	36.57 ^m	−31.36 ^m	−5.86 × 10 ^{−6k}	−27.45 × 10 ^{−10k}	2.42 × 10 ^{−8k}
	Cl [−]	−544.37 ^m	−561.36 ^m	77.29 ^m	−69.42 ^m	22.21 × 10 ^{−6k}	−21.29 × 10 ^{−10k}	4.62 × 10 ^{−8k}
y _{aq} [□]	H ⁺	431.64 ^{d,n}	390.15 ⁿ	−96.62 ^{d,n}	−85.87 ⁿ	−4.50 × 10 ^{−6n,o}	15.00 × 10 ^{−10n,o}	−3.00 × 10 ^{−8n,o}
	Na ⁺	181.21 ^{d,n}	149.91 ⁿ	−76.40 ^{d,n}	−43.84 ⁿ	−5.86 × 10 ^{−6n,o}	−27.45 × 10 ^{−10n,o}	2.42 × 10 ^{−8n,o}
	Cl [−]	−512.80 ^{d,n}	−565.08 ⁿ	−41.09 ^{d,n}	−81.90 ⁿ	22.21 × 10 ^{−6n,o}	−21.29 × 10 ^{−10n,o}	4.62 × 10 ^{−8n,o}
ΔY _{hyd} [□]	H ⁺	−1107.95 ^p	−1136.75 ^p	−96.62 ^{p,q}	−85.87 ^{p,q}	−4.50 × 10 ^{−6o,p}	15.00 × 10 ^{−10o,p}	−3.00 × 10 ^{−8o,p}
	Na ⁺	−427.41 ^p	−450.20 ^p	−76.40 ^{p,q}	−43.84 ^{p,q}	−5.86 × 10 ^{−6o,p}	−27.45 × 10 ^{−10o,p}	2.42 × 10 ^{−8o,p}
	Cl [−]	−316.55 ^p	−328.80 ^p	−41.09 ^{p,q}	−81.90 ^{p,q}	22.21 × 10 ^{−6o,p}	−21.29 × 10 ^{−10o,p}	4.62 × 10 ^{−8o,p}

^aThe parameters reported are the standard (y_g[⊙]) and fixed-point (y_g[□]) molar parameters of the gas-phase ions, the standard (y_{aq}[⊙] or y_{aq}^{⊙*}) and fixed-point (y_{aq}[□]) partial molar parameters of the aqueous ions, and the point-to-point (ΔY_{hyd}[□]) hydration parameters of the ions. The aqueous ion parameters are reported in either the standard (no star superscript) or the density-corrected (star superscript) variants. Values are provided for the free energy G, enthalpy H, entropy S, volume V, heat capacity C_p, volume-compressibility K_T, and volume-expansivity A_p. For the free energy G and enthalpy H, formation parameters (Δ_fy_g[⊙], Δ_fy_g[□], Δ_fy_{aq}[⊙], Δ_fy_{aq}^{⊙*}, and Δ_fy_{aq}[□]) are reported instead of partial molar parameters. The standard hydration parameters of the ions (ΔY_{hyd}[⊙] or ΔY_{hyd}^{⊙*}) are not explicitly reported and can be easily deduced (as y_{aq}^{⊙*} − y_g^{⊙*} or y_{aq}[⊙] − y_g[⊙], respectively). The data refer to the standard pressure P^o = 1 bar, molality b^o = 1 mol kg^{−1}, and temperature T^o = 298.15 K. The formation parameters also refer to an electron standard state defined as the ideal electron gas at temperature T^o with properties calculated according to Fermi–Dirac statistics. Note that the aqueous and hydration parameters reported in this table represent experimentally elusive quantities, and are thus to be considered with some caution.¹¹ ^bFor the free energy G and enthalpy H, formation parameters (Δ_fy_g[⊙], Δ_fy_g[□], Δ_fy_{aq}[⊙], Δ_fy_{aq}^{⊙*}, and Δ_fy_{aq}[□]) are reported instead of partial molar parameters. ^cFrom Table 5.9 in ref 11. ^dUsing molar masses¹⁰³ M of 1.00794, 22.989768, and 35.4527 g mol^{−1} for H⁺, Na⁺, and Cl[−] (values for the elements averaged over the natural isotopic distribution; the small difference between element and ion masses as well as the use of Boltzmann instead of Fermi–Dirac statistics for H⁺ have no influence at the precision of the reported numbers¹¹). ^eEquation 6. ^fEquation 5. ^gConverted from Δ_fy_g[⊙] using the analog of eq 14 for formation parameters (subtraction of Δy_g^{⊙→⊙*} from Table 1). ^hEquation 9. ⁱEquation 8. ^jCalculated from Δ_fy_g[⊙] by addition of ΔY_{hyd}[⊙] from Table 5.26 in ref 11. ^kFrom Table 5.26 in ref 11. ^lConverted from y_{aq}^{⊙*} using eq 25 (addition of Δy_{aq}^{⊙*→⊙} from Table 1). ^mConverted from y_{aq}[⊙] or Δ_fy_{aq}[⊙] using eq 25 or its analog for formation parameters (subtraction of Δy_{aq}^{⊙*→⊙} from Table 1). ⁿConverted from y_{aq}^{⊙*} or Δ_fy_{aq}^{⊙*} using eq 20 or its analog for formation parameters (subtraction of Δy_{aq}^{□→⊙*} from Table 1). ^oFor the volume, volume-compressibility and volume-expansivity, ΔY_{hyd}[□] = y_{aq}[□] − y_g[□]. ^pCalculated using eq 10 or its analog for formation parameters, i.e., as y_{aq}[□] − y_g[□] or Δ_fy_{aq}[□] − Δ_fy_g[□] (these values are essentially identical to the ones found in Table 5.26 of ref 11). ^qFor the entropy and the heat capacity, ΔY_{hyd}[□] = y_{aq}[□].

2.3.1. Method I. In method I, the point-to-point hydration enthalpy ΔH_{hyd}[□] and the fixed-point aqueous partial molar volume ν_{aq}[□] are calculated based on the variations of the average potential energy and box volume, respectively, upon inserting the ion into a pure-liquid sample. Finite-difference analysis of the corresponding values calculated at different pressures P and temperatures T also permits the determination of c_{p, aq}[□], k_{T, aq}[□], and a_{p, aq}[□]. However, the method does not give access to ΔG_{hyd}[□] and s_{aq}[□]. This approach requires two isobaric–isothermal simulations per P, T–point, both involving the same number of water molecules and differing only by the presence or absence of the ion.

Given the variation ΔU of the average potential energy of the system and the corresponding variation ΔV of the average box volume, both assumed to be expressed on a per mole basis, ΔH_{hyd}[□] can be evaluated as

$$\Delta H_{\text{hyd}}^{\square} = \Delta U + P\Delta V \approx \Delta U \quad (27)$$

This equation is only valid for monoatomic species, for which the internal potential energy is zero within the classical model used in the simulations. For polyatomic species, it would have to be corrected by the average intramolecular potential energy

of the species in the gas phase. The equation holds irrespective of whether the species is free or positionally constrained during the simulation. However, if the variation ΔE of the total energy is considered instead of the variation ΔU of the potential energy, a term −(3/2)RT^o must be added to compensate for the average translational kinetic energy of the monoatomic species, unless it is positionally constrained during the simulation. A calculation based on ΔU was preferred in the present work, because it removes the unnecessary noise associated with the kinetic energy fluctuations of the system. The connection between ν_{aq}[□] and ΔV is given by

$$\nu_{\text{aq}}^{\square} = \Delta V \quad (28)$$

This equation is generally valid, i.e., for monoatomic as well as polyatomic species. The neglect of the term PΔV in eq 27 is justified by the very small partial molar volumes of the species considered here. For example, noting that ν_{aq}[□] is on the order of ±3 × 10^{−5} m³ mol^{−1} for Na⁺ and Cl[−] in water (section 4), PΔV is on the order of ±3 × 10^{−3} kJ mol^{−1} at P^o and T^o, which is entirely negligible given the statistical error of the calculations.

Finite-difference expressions for $c_{p,aq}^{\square}$, $k_{T,aq}^{\square}$ and $a_{p,aq}^{\square}$ can be deduced from eq 12 given the forms of the thermodynamic-derivative operators \hat{O}_Y in eq 2, namely

$$c_{p,aq}^{\square} \approx \tilde{\partial}_{\Delta T} \Delta H_{hyd}^{\square}, \quad k_{T,aq}^{\square} \approx -\tilde{\partial}_{\Delta P} v_{aq}^{\square}, \quad \text{and} \quad a_{p,aq}^{\square} \approx \tilde{\partial}_{\Delta T} v_{aq}^{\square} \quad (29)$$

where $\tilde{\partial}_{\Delta Q}$ represents a first-order finite-difference operator for property Q based on an interval ΔQ . For example, for a centered finite difference, one has

$$\tilde{\partial}_{\Delta Q} f(Q, R) = (\Delta Q)^{-1} [f(Q + \Delta Q/2, R) - f(Q - \Delta Q/2, R)] \quad (30)$$

Note that the expression for $c_{p,aq}^{\square}$ in eq 29 relies on the alternative expression for \hat{O}_H in eq 2. This expression is also restricted to monoatomic species (or fully rigid polyatomic species) because it assumes that $c_{p,g}^{\square} = 0$, while those for $k_{T,aq}^{\square}$ and $a_{p,aq}^{\square}$ are generally valid, i.e., for monoatomic as well as rigid or flexible polyatomic species. The neglect of the temperature derivative of the term $P\Delta V$ in eq 27 when evaluating $c_{p,aq}^{\square}$ is justified by the very small partial molar volume-expansivity of the species considered here. For example, noting that $a_{p,aq}^{\square}$ is on the order of $\pm 2 \times 10^{-7} \text{ m}^3 \text{ mol}^{-1} \text{ K}^{-1}$ for Na^+ and Cl^- in water (section 4), $P\partial_T \Delta V$ is on the order of $\mp 2 \times 10^{-2} \text{ J mol}^{-1} \text{ K}^{-1}$ at P° and T° , which is entirely negligible given the statistical error of the calculations.

Equations 27 and 28 are only exact in the limit of infinite dilution, i.e., considering a system including the entire solvation range where the influence of the ion on the potential energy (solvent polarization) and volume (excluded volume, electrostriction) is significant. In practice, this condition is not satisfied for the system sizes considered here (section 3), and corrections for finite-system (as well as approximate-electrostatics) errors must be applied to the raw results, as described in section 2.4. In variant A (section 2.4.1), eq 29 is immediately applied to the raw results of eqs 27 and 28, and the five types of raw variables are corrected subsequently. In variant B (section 2.4.2), the raw results of eqs 27 and 28 are corrected prior to application of eq 29, directly leading to the five types of variables in a corrected form.

2.3.2. Method II. In method II, the point-to-point hydration free energy ΔG_{hyd}^{\square} is calculated on the basis of the reversible work associated with the insertion of the ion into a pure-liquid sample. Finite-difference analysis of the corresponding values calculated at different pressures P and temperatures T also permits in principle the determination of ΔH_{hyd}^{\square} , s_{aq}^{\square} , v_{aq}^{\square} , $c_{p,aq}^{\square}$, $k_{T,aq}^{\square}$ and $a_{p,aq}^{\square}$, i.e., in contrast to method I, the free energy and entropy can also be evaluated. This approach requires two sets of isobaric–isothermal simulations per P, T -point, accounting for the progressive growth of a neutral ion-sized cavity, referred to as the cavitation process, and the progressive increase of the cavity charge from zero to the full ionic charge, referred to as the charging process.

Given the reversible work ΔG_{cav} of cavitation and the reversible work ΔG_{chg} of charging, both assumed to be expressed on a per mole basis, ΔG_{hyd}^{\square} can be evaluated as

$$\Delta G_{hyd}^{\square} = \Delta G_{cav} + \Delta G_{chg} \quad (31)$$

This equation is only valid for monoatomic species, for which the internal potential energy is zero within the classical model used in the simulations. For polyatomic species, it would have to be corrected by the corresponding reversible work in the gas

phase. The equation holds irrespective of whether the species is free or positionally constrained during the simulation because the solvation process involves no change in the atomic mass.

Finite-difference expressions for ΔH_{hyd}^{\square} , s_{aq}^{\square} , v_{aq}^{\square} , $c_{p,aq}^{\square}$, $k_{T,aq}^{\square}$ and $a_{p,aq}^{\square}$ can be deduced from eq 12 given the forms of the thermodynamic-derivative operators \hat{O}_Y in eq 2, namely

$$\begin{aligned} \Delta H_{hyd}^{\square} &\approx (1 - T^{-1} \tilde{\partial}_{\Delta T}) \Delta G_{hyd}^{\square} & s_{aq}^{\square} &\approx -\tilde{\partial}_{\Delta T} \Delta G_{hyd}^{\square} \\ v_{aq}^{\square} &\approx \tilde{\partial}_{\Delta P} \Delta G_{hyd}^{\square} & c_{p,aq}^{\square} &\approx -T^{-1} \tilde{\partial}_{\Delta T}^2 \Delta G_{hyd}^{\square} \\ k_{T,aq}^{\square} &\approx -\tilde{\partial}_{\Delta P}^2 \Delta G_{hyd}^{\square} & a_{p,aq}^{\square} &\approx \tilde{\partial}_{\Delta P, \Delta T}^2 \Delta G_{hyd}^{\square} \end{aligned} \quad (32)$$

where $\tilde{\partial}_{\Delta Q}$ represents a first-order finite-difference operator for property Q based on an interval ΔQ (e.g., eq 30), while $\tilde{\partial}_{\Delta Q}^2$ and $\tilde{\partial}_{\Delta Q, \Delta R}^2$ represent corresponding second-order (self or cross) operators. For example, for centered finite differences, one has

$$\begin{aligned} \tilde{\partial}_{\Delta Q}^2 f(Q, R) &= (\Delta Q/2)^{-2} [f(Q - \Delta Q/2, R) - 2f(Q, R) \\ &\quad + f(Q + \Delta Q/2, R)] \end{aligned} \quad (33)$$

and

$$\begin{aligned} \tilde{\partial}_{\Delta Q, \Delta R}^2 f(Q, R) &= (\Delta Q \Delta R)^{-1} [f(Q - \Delta Q/2, R - \Delta R/2) \\ &\quad + f(Q + \Delta Q/2, R + \Delta R/2) \\ &\quad - f(Q + \Delta Q/2, R - \Delta R/2) \\ &\quad - f(Q - \Delta Q/2, R + \Delta R/2)] \end{aligned} \quad (34)$$

The expressions for ΔH_{hyd}^{\square} , v_{aq}^{\square} , $k_{T,aq}^{\square}$ and $a_{p,aq}^{\square}$ in eq 32 are generally valid, i.e., for monoatomic as well as rigid or flexible polyatomic species, the omission of the terms v_g^{\square} , $k_{T,g}^{\square}$ and $a_{p,g}^{\square}$ being justified by eq 8, although the calculation of ΔG_{hyd}^{\square} itself based on eq 31 is restricted to monoatomic species. The expressions for s_{aq}^{\square} and $c_{p,aq}^{\square}$ however, assume a closed-shell monoatomic species exempt of thermally accessible electronically excited states, in which case of the omission of the terms s_g^{\square} and $c_{p,g}^{\square}$ is justified by eq 9.

Equation 31 is only exact in the limit of infinite dilution, i.e., considering a system including the entire solvation range where the influence of the ion on the potential energy (solvent polarization) and volume (excluded volume, electrostriction) is significant. In practice, this condition is not satisfied for system sizes considered here (section 3), and corrections for finite-system effects (as well as approximate-electrostatics) errors must be applied to the raw results, as described in section 2.4. In variant A (section 2.4.1), eq 32 is immediately applied to the raw results of eq 31, and the seven types of raw variables are corrected subsequently. In variant B (section 2.4.2), the raw results of eq 31 are corrected prior to application of eq 32, directly leading to the seven types of variables in a corrected form.

2.4. Correction Scheme. The raw thermodynamic parameters calculated on the basis of atomistic simulations using methods I or II (section 2.3) are affected by errors related to the finite size of the simulated systems and to the approximate treatment of electrostatic interactions in the simulations. However, the application of an appropriate correction scheme allows for a conversion of the methodology-dependent raw data into methodology-independent results.^{7–11} The corrected values are then exclusively characteristic

of the underlying molecular model and correspond to the idealized situation of an infinite bulk phase exempt of surface polarization, in which electrostatic interactions are exactly Coulombic. In terms of the point-to-point hydration free energy, the application of this correction scheme can be written

$$\Delta G_{\text{hyd}}^{\square} = \Delta G_{\text{hyd,raw}}^{\square} + \Delta G_{\text{cor}}^{\square} \quad (35)$$

The correction term $\Delta G_{\text{cor}}^{\square}$ must account for (see refs 8, 10, and 11 and references therein):

- the deviation of the solvent polarization around the ion relative to the polarization in an ideal Coulombic system and the incomplete or/and inexact interaction of the ion with the polarized solvent, a consequence of possible approximations made in the representation of electrostatic interactions during the simulation (e.g., non-Coulombic interactions involving cutoff truncation)
- the deviation of the solvent polarization around the ion relative to the polarization in an ideal macroscopic system, a consequence of the use of a finite (microscopic and possibly periodic) system during the simulation (e.g., computational box simulated under periodic boundary conditions)
- the deviation of the solvent-generated electrostatic potential at the ion site as calculated from the simulated trajectory relative to the “correct” electrostatic potential, a consequence of the possible application of an inappropriate summation scheme (along with a possibly non-Coulombic potential function) for the contributions of individual solvent atomic charges to this potential, as well as of the possible presence of a constant offset in this potential (e.g., related to the existence of an interfacial potential at the ionic surface along with a constraint of vanishing average potential over the computational box in lattice-sum schemes)
- an inaccurate dielectric permittivity of the employed solvent model

In the context of monoatomic ions, the quantity $\Delta G_{\text{cor}}^{\square}$ in eq 35 generally consists of six terms,⁹ which can be evaluated (either analytically, numerically, or using empirically fitted equations) on the basis of continuum-electrostatics or analytical models. All simulations reported in the present work are performed under periodic boundary conditions based on cubic computational boxes. Except those involved in the calculation of ΔG_{cav} (section 3), for which no correction is required,¹⁰ they rely on a lattice-summation (LS) electrostatic scheme.³⁷ In the specific case of the LS scheme with a cubic box, and considering a water model such as the SPC model¹² characterized by a single van der Waals interaction site, $\Delta G_{\text{cor}}^{\square}$ can be written based on ref 9 (see eq 39 therein)

$$\begin{aligned} \Delta G_{\text{cor}}^{\square} = & \Delta G_{\text{B}}(|q_{\text{I}}|, R_{\text{I}}, M_{\text{W}}, N_{\text{W}}, \rho', \epsilon') \\ & + \Delta G_{\text{C}_1}(q_{\text{I}}, R_{\text{I}}, M_{\text{W}}, N_{\text{W}}, \rho', \gamma') \\ & + \Delta G_{\text{C}_2}(q_{\text{I}}, R_{\text{I}}, M_{\text{W}}, N_{\text{W}}, \rho', \chi', \tilde{\chi}'_{-}) \\ & + \Delta G_{\text{D}}(|q_{\text{I}}|, R_{\text{I}}, \epsilon', \epsilon) \end{aligned} \quad (36)$$

Note the absence of a type-A correction term for the LS scheme, which is formally Coulombic in the limit of infinite box size. The parameters involved in eq 36 are the full ionic charge q_{I} , the effective ionic radius R_{I} , the molar mass M_{W} of water, the number N_{W} of water molecules in the computational box, the

density ρ' of the employed water model, the permittivity ϵ' of the water model, the quadrupole-moment trace γ' of the water model relative to its single van der Waals interaction site, the air–liquid interfacial potential χ' (air-to-liquid direction) of the water model, and its dependence $\tilde{\chi}'_{-}$ on the inverse curvature radius for a concave interface, as well as the experimental solvent permittivity ϵ . The values for the parameters R_{I} , ρ' , ϵ' , χ' , $\tilde{\chi}'_{-}$, and ϵ must be selected as appropriate for $P^{\circ} = 1$ bar and $T^{\circ} = 298.15$ K, i.e., the conditions defining the reference state point for $\Delta G_{\text{hyd}}^{\square}$. Note that the correction is to be applied to raw charging free energies excluding the contribution of the LS self-energy term.

The parameter dependences of the terms in eq 36 have been slightly altered compared to ref 9, namely, the box-edge length L has been expanded in terms of the equilibrium density ρ' of the water model (neglecting the effect of electrostriction), the molar mass M_{W} of water, the number of water molecules N_{W} in the box, and the effective ionic radius R_{I} as

$$L = \left(\frac{N_{\text{W}}M_{\text{W}}}{N_{\text{A}}\rho'} + \frac{4\pi}{3}R_{\text{I}}^3 \right)^{1/3} \quad (37)$$

The exact functional form and the physical interpretation of the terms occurring in eq 36, as well as the procedure to evaluate them, are described in detail elsewhere,⁹ and this information will not be repeated here. The equations used in the present work are merely reported below, for the sake of reproducibility.

The term ΔG_{B} is given by

$$\begin{aligned} \Delta G_{\text{B}} = & (8\pi\epsilon_0)^{-1}N_{\text{A}}q_{\text{I}}^2[1 - (\epsilon')^{-1}]L^{-1} \left[\alpha_{\text{LS}} + \frac{4\pi}{3} \left(\frac{R_{\text{I}}}{L} \right)^2 \right. \\ & \left. - \frac{16\pi^2}{45} \left(\frac{R_{\text{I}}}{L} \right)^5 \right] \end{aligned} \quad (38)$$

where $\alpha_{\text{LS}} \approx -2.837297$ is the LS self-term constant for a cubic box, and L is given by eq 37. The term ΔG_{C_1} is given by

$$\Delta G_{\text{C}_1} = -N_{\text{A}}q_{\text{I}} \left(1 - \frac{4\pi R_{\text{I}}^3}{3L^3} \right) \xi' \quad (39)$$

where L is given by eq 37 and ξ' is the exclusion potential of the solvent model at density ρ' , defined as

$$\xi' = (6\epsilon_0)^{-1}N_{\text{A}}M_{\text{W}}^{-1}\rho'\gamma' \quad (40)$$

ϵ_0 being the permittivity of vacuum. Inserting eqs 37 and 40, eq 39 can be simplified to

$$\Delta G_{\text{C}_1} = -N_{\text{A}}(6\epsilon_0)^{-1}N_{\text{W}}\gamma'q_{\text{I}}L^{-3} \quad (41)$$

The term ΔG_{C_2} is given by

$$\Delta G_{\text{C}_2} = -N_{\text{A}}q_{\text{I}} \frac{4\pi R_{\text{I}}^3}{3L^3} (\chi' + \tilde{\chi}'_{-}R_{\text{I}}^{-1}) \quad (42)$$

where L is given by eq 37. Finally, the term ΔG_{D} is given by

$$\Delta G_{\text{D}} = (8\pi\epsilon_0)^{-1}N_{\text{A}}q_{\text{I}}^2[\epsilon^{-1} - (\epsilon')^{-1}]R_{\text{I}}^{-1} \quad (43)$$

The correction scheme of eq 35 can be generalized to derivative hydration parameters and aqueous partial molar properties, as

$$\Delta Y_{\text{hyd}}^{\square} = \Delta Y_{\text{hyd,raw}}^{\square} + \Delta Y_{\text{cor}}^{\square} \quad (44)$$

and

$$\gamma_{\text{aq}}^{\square} = \gamma_{\text{aq,raw}}^{\square} + \Delta Y_{\text{cor}}^{\square} \quad (45)$$

respectively. The correction term $\Delta Y_{\text{cor}}^{\square}$ is the same in both cases considering that there is no error on the gas-phase properties. These generalized correction terms are given by

$$\Delta Y_{\text{cor}}^{\square} = \hat{O}_Y \Delta G_{\text{cor}}^{\square} \quad (46)$$

In principle, $\Delta Y_{\text{cor}}^{\square}$ can be formulated analytically for all thermodynamic parameters considered here, based on explicit differentiation of the terms contributing to eq 36 as defined by eqs 37, 38, 41, 42, and 43. The resulting expressions are, however, relatively cumbersome, especially for second derivatives.⁹ For this reason, in the present work, the quantities $\Delta Y_{\text{cor}}^{\square}$ are determined in practice by finite-difference analysis of these terms on the basis of very small variations of P and T , the corresponding intervals being sufficiently small for the resulting estimates to be considered indistinguishable from the analytical ones, yet sufficiently large to prevent the occurrence of numerical errors (section 3.4). Irrespective of whether an analytical or a numerical approach is selected, the evaluation of the correction terms $\Delta Y_{\text{cor}}^{\square}$ requires knowledge of the first and second (self and cross) derivatives of the involved parameters (R_{f} , ρ' , ϵ' , χ' , $\tilde{\chi}'$, and ϵ) with respect to temperature and pressure at P° and T^{-} . Note that M_{W} and γ' are constants, independent of pressure and temperature.

For both methods I and II (section 2.3), two alternative variants are considered for the application of the correction scheme to derivative thermodynamic properties, referred to here as variants A and B.

2.4.1. Variant A. In variant A, the raw values from the simulations are corrected after application of finite difference in pressure or/and temperature, based on correction terms specifically designed for derivative parameters at P° and T^{-} according to eq 46. For method I (section 2.3.1), this implies that the five raw quantities $\Delta H_{\text{hyd,raw}}^{\square}$, $v_{\text{hyd,raw}}^{\square}$, $c_{\text{P,hyd,raw}}^{\square}$, $k_{\text{T,hyd,raw}}^{\square}$, and $a_{\text{P,hyd,raw}}^{\square}$ are calculated by means of eqs 27–29 and subsequently corrected using eqs 44 or 45. For method II (section 2.3.2), this implies that the seven raw quantities $\Delta G_{\text{hyd,raw}}^{\square}$, $\Delta H_{\text{hyd,raw}}^{\square}$, $s_{\text{hyd,raw}}^{\square}$, $v_{\text{hyd,raw}}^{\square}$, $c_{\text{P,hyd,raw}}^{\square}$, $k_{\text{T,hyd,raw}}^{\square}$, and $a_{\text{P,hyd,raw}}^{\square}$ are calculated by means of eqs 31 and 32 and subsequently corrected using eqs 44 or 45. Because only the correction terms $\Delta Y_{\text{cor}}^{\square}$ appropriate for P° and T^{-} are employed, variant A only requires knowledge of the first and second (self and cross) derivatives of the involved parameters (R_{f} , ρ' , ϵ' , χ' , $\tilde{\chi}'$, and ϵ) with respect to pressure and temperature at P° and T^{-} but not of their full functional dependence on P and T . Arguments in favor of variant A are that it requires less information on the input parameters of the correction scheme (derivatives at P° and T^{-} , rather than full functional dependence on P and T) and that it involves an exact evaluation of the correction terms at P° and T^{-} (rather than a finite-difference approximation to these terms).

2.4.2. Variant B. In variant B, the raw values from the simulations are corrected prior to application of finite difference in pressure or/and temperature, based on corresponding correction terms appropriate for the different simulation pressures and temperatures P and T considered, i.e., according to analogs of eq 46 at P, T -points differing from P° and T^{-} . For method I (section 2.3.1), this implies that the raw quantities $\Delta H_{\text{hyd,raw}}(P, T)$ and $v_{\text{aq,raw}}(P, T)$ are calculated by means of equations analogous to eqs 27 and 28 at all required P, T -points, corrected to $\Delta H_{\text{hyd}}(P, T)$ and $v_{\text{aq}}(P, T)$ by equations analogous

to eqs 44 or 45 at the corresponding P, T -point, and subsequently entered into the finite-difference scheme of eq 29. For method II (section 2.3.2), this implies that the raw quantity $\Delta G_{\text{hyd,raw}}(P, T)$ is calculated by means of an equation analogous to eq 31 at all required P, T -points, corrected to $\Delta G_{\text{hyd}}(P, T)$ by an equation analogous to eq 35 at the corresponding P, T -point, and subsequently entered into the finite-difference scheme of eq 32. Because correction terms $\Delta Y_{\text{cor}}(P, T)$ at different P, T -points are employed, variant B requires knowledge of the full functional dependence of the involved parameters (R_{f} , ρ' , ϵ' , χ' , $\tilde{\chi}'$, and ϵ) with respect to pressure and temperature. Compared to variant A, this variant thus requires more information on the input parameters of the correction scheme (full functional dependence on P and T , rather than only derivatives at P° and T^{-}) and involves an approximate evaluation of the correction terms at P° and T^{-} (finite-difference approximation to these terms). However, an argument in favor of variant B is that the finite-difference errors (effect of nonlinear contributions) committed in the evaluation of the raw derivative parameters may be partially canceled out by corresponding finite-difference errors in the evaluation of the correction terms.

3. COMPUTATIONAL DETAILS

3.1. Simulation Parameters. All MD simulations required for the application of method I (section 2.3.1) and for the evaluation of the charging component in method II (section 2.3.2) were carried out using a modified version of the GROMOS96 program^{38,39} implementing the particle-particle particle-mesh (P³M) LS method^{37,40} for calculating the electrostatic interactions. The MD simulations required for the evaluation of the cavitation component in method II were carried out using the GROMOS05 program⁴¹ and relied on a molecule-based cutoff-truncation scheme with a Barker–Watts reaction-field (RF) correction⁴² for calculating the electrostatic interactions. The use of the RF scheme in the latter case is motivated by a lower computational cost and by the limited sensitivity of the cavitation free energy on the selected electrostatic scheme observed in ref 10 (see, e.g., Supporting Information Table S2.Ib therein).

The simulations were performed under periodic boundary conditions based on cubic computational boxes containing 512 (method I only), 724, or 1024 simple point charge¹² (SPC) water molecules. Depending on the calculation, the box possibly also contained a single Na⁺ ion or a single Cl[−] ion. The corresponding ion–solvent Lennard-Jones interaction parameters were taken from set L in ref 10 (see Tables II and III therein). The equations of motion were integrated using the leapfrog scheme⁴³ with a time step of 2 fs. The rigidity of the water molecules was enforced by application of the SHAKE procedure⁴⁴ with a relative geometric tolerance of 10^{−4}. The center of mass translation of the computational box was removed every 2 ps. All simulations were performed at constant pressure and temperature. The pressure was maintained close to its reference value P by weak coupling⁴⁵ to a pressure bath (isotropic coordinate scaling) using a value of 7.513 × 10^{−4} kJ^{−1} mol nm³ for the isothermal compressibility of water⁴⁶ and a coupling time of 0.5 ps. The temperature was maintained close to its reference value T by weak coupling⁴⁵ to a temperature bath using a coupling time of 0.1 ps.

The LS scheme (method I and charging component of method II) was applied with tinfoil boundary conditions using^{37,40,47,48} a spherical hat charge-shaping function of width

1.0 nm, a triangular shaped cloud assignment function, a finite-difference scheme of order 2, and grid spacings of about 0.08, 0.09, or 0.10 nm for the systems involving 512, 724, and 1024 water molecules, respectively. This choice of parameters led to a ratio of the root-mean square error in the atomic forces to the average norm of these forces^{37,48–50} of about 0.02–0.05% for the different systems. The LS self-energy term^{37,51–54} was removed in the calculation of the total potential energy and of the electrostatic potential at the ion site. A pressure correction was applied so as to remove the effect of this self-energy term on the virial, as described by Bogusz et al.⁵⁵ Although the application of the latter correction is of limited importance when calculating ionic solvation free energies,¹⁰ it turns out to be essential for the accurate evaluation of ionic partial molar volumes and their derivatives (data not shown). The nonbonded pairlist was updated every time step, and the Lennard-Jones interactions were truncated at a distance of 1.0 nm.

The RF scheme (cavitation component of method II) was applied using a molecule-based cutoff distance of 1.4 nm and a reaction-field permittivity of 66.6 as appropriate⁵⁶ for the SPC water model. The nonbonded pairlist was updated every time step, and the Lennard-Jones interactions were truncated at a distance of 1.4 nm. Only computational boxes containing 724 or 1024 water molecules were considered here, the box containing 512 molecules being too small for the selected cutoff distance.

For the estimation of derivative properties by finite difference, pressure increments of 5000 bar and temperature increments of 25 K (method I) or 12.5 K (method II), respectively, were employed. The choice of these relatively large pressure increments is motivated by the magnitude of the ionic partial molar volumes, on the order of $10^{-5} \text{ m}^3 \text{ mol}^{-1}$ (section 4), requiring a pressure change of 1000 bar = 10^8 J m^{-3} for a change in free energy of about 1 kJ mol^{-1} , i.e., measurable with a sufficient precision in the present calculations.

The experimental data against which the calculation results were compared (in terms of point-to-point or fixed-point parameters) is summarized in Table 2. The three following sections provide further details on the application of method I, of method II, and of the correction scheme within the two methods.

3.2. Method I. The application of method I relied on five sets of nine calculations, each set involving simulations of the water box (512, 724, or 1024 molecules) either in the absence or in the presence of one ion (Na^+ or Cl^-). The five sets corresponded to a pressure $P = 1$ bar along with temperatures T of 273.15, 298.15, or 323.15 K, and to a temperature $T = 298.15$ K along with pressures P of 1, 5000, or 10000 bar. The 45 simulations, relying on LS electrostatics, were carried out for a period of 30 ns (at 5000 and 10000 bar) or 60 ns (at 1 bar) after 0.1 ns equilibration. The total potential energy (exempt of LS self-energy term) was written to file every 0.2 ps and the box volume every 2 fs.

The raw point-to-point hydration enthalpy $\Delta H_{\text{hyd}}^{\square}$ and fixed-point aqueous partial molar volume v_{aq}^{\square} were calculated according to eqs 27 and 28, respectively, based on the simulations at 1 bar and 298.15 K. Errors in the individual ensemble averages for the total potential energy and box volume were calculated by block-averaging⁵⁷ and propagated into an error estimate for $\Delta H_{\text{hyd}}^{\square}$ and v_{aq}^{\square} , respectively, by taking the square-root of the sum of the squared errors corresponding to the simulations in the absence or presence of the ion. The

fixed-point aqueous partial molar heat capacity $c_{p,\text{aq}}^{\square}$ and volume-expansivity $\alpha_{p,\text{aq}}^{\square}$ were calculated according to eq 29 using a centered finite difference (eq 30) based on the simulations at 1 bar and 273.15 or 323.15 K. The fixed-point aqueous partial molar volume-compressibility $k_{T,\text{aq}}^{\square}$ was calculated according to eq 29 based on the simulations at 298.15 K and 1, 5000, or 10000 bar. Since the use of a negative pressure of -5000 bar led to cavitation in the simulated systems (data not shown), the application of a centered finite difference (eq 30) was not possible here, and $\partial_{\Delta p} v_{\text{aq}}^{\square}$ in eq 29 was evaluated instead as the slope of a straight line fitted to the pressure dependence of the partial molar volume. For the determination of corrected $c_{p,\text{aq}}^{\square}$, $k_{T,\text{aq}}^{\square}$, and $\alpha_{p,\text{aq}}^{\square}$ values, the correction scheme was applied either before or after differentiation in variants A and B, respectively (there is no such distinction for $\Delta H_{\text{hyd}}^{\square}$ and v_{aq}^{\square}). Errors on $c_{p,\text{aq}}^{\square}$ and $\alpha_{p,\text{aq}}^{\square}$ were estimated by taking the square-root of the sum of the squared errors in $\Delta H_{\text{hyd}}^{\square}$ and v_{aq}^{\square} , respectively, corresponding to the simulations at 273.15 and 323.15 K, and dividing by the temperature interval of 50 K. Errors on $k_{T,\text{aq}}^{\square}$ were estimated by propagating analytically⁵⁸ the individual errors in the partial molar volumes onto the slope of the fitted line representing the pressure dependence of the partial molar volume.

3.3. Method II. The application of method II relied on seven sets of eight (or four) calculations, each set involving the evaluation of two free-energy differences (charging and cavitation) for a given ion (Na^+ or Cl^-) and considering systems involving either 724 or 1024 (or only 1024) water molecules. The seven sets corresponded to a pressure $P = 1$ bar along with temperatures T of 273.15, 285.65, 298.15, 310.65, or 323.15 K, and to a temperature $T = 298.15$ K along with pressures P of 1, 5000, or 10000 bar, the two latter sets only considering systems involving 1024 water molecules.

The 24 calculations of cavitation free energies ΔG_{cav} carried out using RF electrostatics, relied on thermodynamic integration⁵⁹ over the derivative of the Hamiltonian with respect to a scaling parameter λ applied to the ion–water Lennard-Jones interaction of the uncharged ion, from no interaction at $\lambda = 0$ to full interaction at $\lambda = 1$. The λ coupling was chosen to be quadratic and involved a soft-core scaling³⁸ with $\alpha_{\text{LJ}} = 0.5$. The calculation relied on 28 λ points (spacing of 0.05, decreased to 0.01 between 0.45 and 0.55 due to a sharper variation of the Hamiltonian derivative near 0.5), and the integration was performed using the trapezoidal rule. At each λ point, the simulation was carried out for a period of 2 ns after 0.1 ns equilibration, and the Hamiltonian derivative was written to file every 0.2 ps. Errors in the individual ensemble averages for the Hamiltonian derivative were calculated by block-averaging⁵⁷ and propagated into an error estimate for ΔG_{cav} according to the trapezoidal rule.

The 24 calculations of raw charging free energies ΔG_{chg} carried out using LS electrostatics, relied on a scheme introduced by Hummer et al.⁵³ In this scheme, closely related to thermodynamic integration,⁵⁹ the averages and fluctuations of the solvent-generated electrostatic potential at the ion site are recorded for different ionic charge states q_1' , from zero to the full ionic charge q_1 . This information is used to construct an optimal free-energy profile, from which the free-energy difference is then extracted. The calculation relied on three charge states ($q_1'/q_1 = 0.0, 0.5$, and 1.0), which is sufficient considering that the free-energy profiles are very close to quadratic for monovalent ions in water (Born model⁶⁰). At each q_1' point, the simulation was carried out for a period of

1 ns after 0.1 ns equilibration, and the instantaneous solvent-generated potential (exempt of LS self-energy term contribution) was written to file every time step (2 fs). Errors in the individual ensemble averages for the solvent-generated potential were calculated by block-averaging⁵⁷ and propagated into an error estimate for ΔG_{chg} according to the trapezoidal rule.

The raw point-to-point hydration free energy $\Delta G_{\text{hyd}}^{\square}$ was calculated according to eq 31 based on the simulations at 1 bar and 298.15 K. The point-to-point hydration enthalpy $\Delta H_{\text{hyd}}^{\square}$ and fixed-point aqueous partial molar entropy s_{aq}^{\square} were calculated according to eq 29 based on the simulations at 1 bar and 273.15, 285.65, 298.15, 310.65, or 323.15 K. For increased accuracy, $\partial_{\Delta T} \Delta G_{\text{hyd}}^{\square}$ in eq 32 was not evaluated by centered finite difference (eq 30) but as the slope of a straight line fitted to the temperature dependence of the hydration free energy, considering separate fits for cavitation and raw (variant A) or corrected (variant B) charging contributions, respectively. The fixed-point aqueous partial molar volume v_{aq}^{\square} was calculated according to eq 32 based on the simulations at 298.15 K and 1, 5000, or 10 000 bar. Here also, $\partial_{\Delta P} \Delta G_{\text{hyd}}^{\square}$ in eq 32 was evaluated as the slope of a straight line fitted to the pressure dependence of the hydration free energy, considering separate fits for cavitation and raw (variant A) or corrected (variant B) charging contributions, respectively. The evaluation of the quantities $\partial_{\Delta P}^2 \Delta G_{\text{hyd}}^{\square}$, $\partial_{\Delta T}^2 \Delta G_{\text{hyd}}^{\square}$ and $\partial_{\Delta P, \Delta T}^2 \Delta G_{\text{hyd}}^{\square}$ in eq 32 could not be performed with sufficient accuracy for an evaluation of the fixed-point aqueous partial molar heat capacity $c_{p, \text{aq}}^{\square}$, volume-compressibility $k_{T, \text{aq}}^{\square}$ and volume-expansivity $\alpha_{P, \text{aq}}^{\square}$ via method II. It was nevertheless checked that the estimates for these quantities obtained via method I are compatible with the curvature of $\Delta G_{\text{hyd}}^{\square}$ as a function of pressure or/and temperature, given the associated uncertainty (section 4.2.3). For the determination of corrected $\Delta H_{\text{hyd}}^{\square}$, s_{aq}^{\square} and v_{aq}^{\square} values, the correction scheme was applied either before or after differentiation in variants A and B, respectively (there is no such distinction for $\Delta G_{\text{hyd}}^{\square}$).

The square root of the sum of squared errors on ΔG_{cav} and ΔG_{chg} (see above) was used as an estimate for the corresponding error on the hydration free energy. Errors on s_{aq}^{\square} and v_{aq}^{\square} were estimated by propagating analytically⁵⁸ the individual errors in the free energies onto the slope of the fitted lines representing the temperature or pressure dependence of the hydration free energy, respectively. Errors on $\Delta H_{\text{hyd}}^{\square}$ were estimated by propagating the errors on $\Delta G_{\text{hyd}}^{\square}$ and s_{aq}^{\square} via the Gibbs equation.

3.4. Correction Scheme. The correction term $\Delta G_{\text{cor}}^{\square}$ defined by eq 36 is to be applied to raw charging free energies excluding the contribution of the LS self-energy term and consists of four terms that are functions of nine parameters, based on the expressions of eqs 37, 38, 41, 42, and 43. For those parameters depending on P and T , the corresponding values must be selected as appropriate for $P^{\circ} = 1$ bar and $T^{-} = 298.15$ K. The values selected in the present work are $q_{\text{I}} = +1.0$ or $-1.0e$ for Na^{+} and Cl^{-} , respectively; $R_{\text{I}} = 0.168$ or 0.246 nm for Na^{+} and Cl^{-} , respectively (effective radius R_{mean} , based on ref 10); $N_{\text{W}} = 512$, 724, or 1024 (depending on the simulated system); $\rho' = 968.2$ kg m⁻³ (SPC water model, based on the simulations carried out in the present work); $\epsilon' = 66.6$ (SPC water model, based on ref 56); $\gamma' = 8.2 \times 10^{-3} e$ nm² (SPC water model, analytical, see e.g. refs 7, 9, and 11); $\chi' = 0.73$ V (SPC water model, based on ref 7); $\tilde{\chi}' = -0.11$ V nm (SPC

water model, based on ref 7); and $\epsilon = 78.4$ (experimental, based on ref 61).

The box-edge length L of the system does not enter explicitly into the correction scheme but is derived here from R_{I} , N_{W} , and ρ' according to eq 37 (using $M_{\text{W}} = 0.018015$ kg mol⁻¹). The resulting values are $L = 2.51$, 2.82, or 3.16 nm for $N_{\text{W}} = 512$, 724, and 1024, respectively. Similarly, the exclusion potential ξ' of the solvent model is not an explicit parameter of the scheme. It is defined by eq 40 and evaluates to $\xi' = 0.80$ V for the SPC water model at P° and T^{-} with an “accurate” electrostatic scheme (the scheme may have a slight influence on ξ' via ρ').

The corresponding correction terms $\Delta Y_{\text{cor}}^{\square}$ for derivative properties at P° and T^{-} are defined by eq 46. As mentioned in section 2.4, the resulting analytical expressions are relatively cumbersome.⁹ For this reason, in the present work, the quantities $\Delta Y_{\text{cor}}^{\square}$ were determined by finite-difference analysis of eq 36 based on very small variations of P and T . In practice, a grid-based finite-difference formula⁶² was applied considering 121 values of ΔG_{cor} corresponding to 11 equispaced temperatures ($\Delta T = 3$ K) and pressures ($\Delta P = 0.1$ bar) around P° and T^{-} . This evaluation requires knowledge of the first and second (self and cross) derivatives of the nine parameters of the scheme with respect to pressure and temperature at P° and T^{-} (see further below).

The quantities $\Delta Y_{\text{cor}}^{\square}$ at P° and T^{-} , including $\Delta G_{\text{cor}}^{\square}$, are sufficient to calculate all correction terms when applying variant A of the correction scheme (section 2.4.1). However, when applying variant B (section 2.4.2), it is necessary to evaluate $\Delta G_{\text{cor}}(P, T)$ in eq 36 and $\Delta Y_{\text{cor}}(P, T)$ in eq 46 at pressures P and temperatures T differing from P° and T^{-} . Here also, $\Delta Y_{\text{cor}}(P, T)$ is obtained from a grid-based finite-difference formula,⁶² applied considering 121 values of ΔG_{cor} around the selected P, T -point. Clearly, however, the evaluation of the quantities $\Delta Y_{\text{cor}}(P, T)$, including $\Delta G_{\text{cor}}(P, T)$, requires knowledge of the full pressure and temperature dependences of the nine parameters of the scheme.

The parameters q_{I} , N_{W} , and γ' are independent of pressure and temperature. The parameters R_{I} , χ' , and $\tilde{\chi}'$ were assumed to be linearly dependent on temperature (slopes from ref 9) and independent of pressure. The relative dependences of the density ρ' and permittivity ϵ' of the solvent model on pressure and temperature were taken from experimentally parametrized curves for water. More specifically, $\rho'(P, T)$ was calculated as

$$\rho'(P, T) = \frac{\rho'^{\ominus}}{\rho^{\ominus}} \rho(P, T) \quad (47)$$

where $\rho(R, T)$ denotes the experimental density of water at P and T according to the IAPWS-95 parametrization,⁶³ and $\epsilon'(P, T)$ was calculated as

$$\epsilon'(P, T) = \frac{\epsilon'^{\ominus}}{\epsilon^{\ominus}} \epsilon(P, T) \quad (48)$$

where $\epsilon(P, T)$ denotes the experimental permittivity of water at P and T according to the Bradley and Pitzer parametrization.⁶¹ The same parametrization was employed for the experimental solvent permittivity $\epsilon(P, T)$, which is also a parameter of the correction scheme. The expression for $\epsilon(P, T)$ is provided explicitly in section S.I of the Supporting Information document. The calculation of $\rho(P, T)$ was performed using available IAPWS software.⁶⁴ For all of the other parameters, function values and derivatives at P° and T^{-} are sufficient to

Table 3. Parameters Used in the Application of the Correction Scheme^a

parameter	unit (u)	f [u]	∂_{Tf} [u K ⁻¹]	$\partial_{T^2}^2 f$ [u K ⁻²]	∂_{Pf} [u bar ⁻¹]	$\partial_{P^2}^2 f$ [u bar ⁻²]	$\partial_{P,T}^2 f$ [u bar ⁻¹ K ⁻¹]
$R_i(\text{Na}^+)^{b,c,d}$	m	1.68×10^{-10}	-4×10^{-14}	0	0	0	0
$R_i(\text{Cl}^-)^{b,c}$	m	2.46×10^{-10}	-4×10^{-14}	0	0	0	0
$\rho^{d,e}$	kg m ⁻³	9.9705×10^2	-2.57×10^{-1}	-9.53×10^{-3}	4.51×10^{-2}	-9.56×10^{-6}	-1.23×10^{-4}
$\rho'^{d,f}$	kg m ⁻³	9.682×10^2	-2.49×10^{-1}	-9.26×10^{-3}	4.38×10^{-2}	-9.28×10^{-6}	-1.19×10^{-4}
$\epsilon^{d,g}$	1	7.8384×10^1	-3.5930×10^{-1}	1.5526×10^{-3}	3.7055×10^{-3}	-5.4964×10^{-7}	-9.9103×10^{-6}
$\epsilon'^{d,h}$	1	6.66×10^1	-3.0522×10^{-1}	1.3190×10^{-3}	3.1478×10^{-3}	-4.6691×10^{-7}	-8.4187×10^{-6}
$\chi'^{c,i}$	V	7.3×10^{-1}	-4.8×10^{-4}	0	0	0	0
$\tilde{\chi}'^{c,i}$	V m	-1.10×10^{-10}	-6.72×10^{-14}	0	0	0	0
$\tilde{\chi}'^{c,i,j}$	V m	-1.11×10^{-9}	-7.3×10^{-13}	0	0	0	0

^aThese parameters enter into the evaluation of $\Delta G_{\text{cor}}^{\square}$ (eq 36) and are the effective ionic radius R_i , the density ρ' of the employed water model, the permittivity ϵ' of the water model, the air–liquid interfacial potential χ' (air-to-liquid direction) of the water model and its dependence $\tilde{\chi}'$ on the inverse curvature radius for a concave interface, as well as the experimental solvent permittivity ϵ . Additional entries for the experimental solvent density ρ are also included. The corresponding first and second (self and cross) derivatives (∂_P , ∂_T , ∂_P^2 , ∂_T^2 , and $\partial_{P,T}^2$) with respect to pressure P or/and temperature T are also reported. The data refer to the SPC water model and the Na^+ and Cl^- ions of set L in ref 10, as well as to the standard pressure $P^\circ = 1$ bar and temperature $T^\circ = 298.15$ K. This information entirely defines the correction scheme for variant A. It must be complemented by the functional dependence of ρ and ϵ for variant B. ^bValue from ref 10 (entry R_{mean} in Tables II and III therein) and estimated temperature derivative from ref 9 (see Table VI therein). ^cSecond temperature derivative as well as pressure dependence neglected due to lack of data, as in ref 9. ^dDiffers slightly from the parameters of ref 9 (see Table VI therein), due to the use of different source data or approximations. ^eBased on the IAPWS-95 parametrization. ^fDensity based on the present simulations, derivatives approximated by means of eq 47, i.e. calculated from those of ρ using a scaling factor of $0.971 = 968.2/997.05$. ^gBased on the Bradley and Pitzer parametrization⁶¹ (Section S.1 of the Supporting Information document). ^hPermittivity based on ref 56, derivatives approximated by means of eq 48, i.e., calculated from those of ϵ using a scaling factor of $0.849 = 66.6/78.384$. ⁱValue and estimated temperature derivative from ref 9 (see Table VI therein), based on ref 7. ^jReported for completeness (value for a convex interface), not necessary in the case of LS simulations (present work).

characterize the correction scheme for both variants A and B. These quantities are reported in Table 3.

4. RESULTS AND DISCUSSION

4.1. Method I. The $\Delta H_{\text{hyd}}^{\square}$, $\nu_{\text{aq}}^{\square}$, $c_{\text{P, aq}}^{\square}$, $k_{\text{T, aq}}^{\square}$, and $a_{\text{P, aq}}^{\square}$ estimates obtained using method I (sections 2.3.1 and 3.2) considering three different system sizes (512, 724, or 1024 water molecules) for the Na^+ or Cl^- ions are reported in Tables 4 and 5, respectively. More details on the calculations can also be found in Tables S.2 and S.3 as well as Figure S.1 of the Supporting Information document. The results for variants A (section 2.4.1) and B (section 2.4.2) are discussed separately in the two following sections.

4.1.1. Variant A. For both Na^+ and Cl^- , the raw hydration enthalpy is negative and increases in magnitude with increasing system size, which indicates that the systems considered fail to encompass a sufficient volume of correctly polarized solvent around the ion. For both ions, this finite-size effect is slightly overcompensated by the type-B correction, leading to corrected hydration enthalpies $\Delta H_{\text{hyd}}^{\square}$ that slightly decrease in magnitude with increasing system size, evaluating to about -476 kJ mol⁻¹ and -365 kJ mol⁻¹ for Na^+ and Cl^- , respectively, considering the largest system. In both cases, the type-B correction for finite-size effects (on the order of -60 to -80 kJ mol⁻¹) is very large for the truly microscopic system sizes considered, which remain very far from a bulk (infinite-dilution) situation. Note also the important contribution of the type-C₁ correction for improper potential summation to these estimates, of comparable magnitude (about 83 kJ mol⁻¹) but opposite sign for the two ions.

The raw partial molar volumes are positive for the two ions and decrease with increasing system size. This trend is also easily understood considering that the positive excluded-volume contribution to this parameter is short-ranged, while the negative electrostrictive contribution is longer-ranged. This finite-size effect is appropriately removed by the type-B correction, leading to corrected partial molar volumes $\nu_{\text{aq}}^{\square}$ that

are essentially identical within the statistical uncertainty (about 1×10^{-6} m³ mol⁻¹) for the three system sizes considered, evaluating to about -33×10^{-6} or $+39 \times 10^{-6}$ m³ mol⁻¹ for Na^+ and Cl^- , respectively. The type-B correction (on the order of -10×10^{-6} m³ mol⁻¹) is again large for both ions but comparatively less important than for the hydration enthalpy. Note again the very large contribution of the type-C₁ correction to these estimates, of comparable magnitude (about 35×10^{-6} m³ mol⁻¹) but opposite sign for the two ions.

The raw partial molar heat capacities are affected by very large statistical uncertainties, suggesting that much longer ($\gg 60$ ns) simulations would be required to achieve proper convergence. This is easily understood considering that method I involves in this case the comparison of two very large numbers, namely, the total potential energies of two aqueous systems including or excluding the ion. Although an uncertainty of about 1 kJ mol⁻¹ on these two numbers is perfectly acceptable in terms of the calculated hydration enthalpy, for a heat capacity evaluated by finite difference over a temperature interval of 50 K, it already leads to an error of about 40 J mol⁻¹ K⁻¹. For Na^+ and Cl^- , the corrected partial molar heat capacities $c_{\text{P, aq}}^{\square}$ obtained for the systems involving 512 and 724 water molecules are very close. For this reason, and because a better convergence of the total potential energy is likely to be achieved for a smaller system, the results obtained using 512 water molecules are considered here to be the most reliable. The suggested $c_{\text{P, aq}}^{\square}$ values are thus about -339 or $+184$ J mol⁻¹ K⁻¹ for Na^+ and Cl^- , respectively, with a large statistical uncertainty (about 30 J mol⁻¹ K⁻¹). The type-B correction (on the order of -60 to -80 J mol⁻¹ K⁻¹) is very large for both ions, as was the case for the hydration enthalpy. However, the type-C₁ correction is even more important here, and again of comparable magnitude (about 220 J mol⁻¹ K⁻¹) but opposite sign for the two ions.

The raw partial molar volume-compressibilities are of opposite signs for the two ions, and tendentially decrease with increasing system size. Note that slightly lower raw values

Table 4. Raw Simulation Data, Correction Terms and Corrected Results Corresponding to Hydration and Aqueous Partial Molar Parameters for Na⁺ Calculated *via* Method I, along with Variants A or B^a

parameter	N_W	L [nm]	correction terms						result	
			ΔY_A	ΔY_B	ΔY_{C_1}	ΔY_{C_2}	ΔY_D	$\Delta Y_{\text{cor}}^{\square}$	$\Delta Y_{\text{hyd,raw}}^b$	ΔY_{hyd}^b
Variant A										
ΔH [kJ mol ⁻¹]	512	2.51	0.0	-80.3	-83.0	0.0	0.4	-162.9	-318.5 ± 0.9	-481.4 ± 0.9
	724	2.82	0.0	-71.6	-83.1	0.0	0.4	-154.3	-324.1 ± 1.0	-478.4 ± 1.0
	1024	3.16	0.0	-63.9	-83.1	0.0	0.4	-146.6	-329.7 ± 1.1	-476.3 ± 1.1
ν [10 ⁻⁶ m ³ mol ⁻¹]	512	2.51	0.0	-12.0	-34.9	0.0	0.4	-46.4	12.9 ± 0.6	-33.4 ± 0.6
	724	2.82	0.0	-10.7	-34.9	0.0	0.4	-45.2	11.9 ± 0.6	-33.2 ± 0.6
	1024	3.16	0.0	-9.6	-34.9	0.0	0.4	-44.0	10.8 ± 0.8 ^c	-33.2 ± 0.8 ^c
c_p [J mol ⁻¹ K ⁻¹]	512	2.51	0.0	-79.8	-219.6	0.0	6.8	-292.5	-46.4 ± 28.4	-339.0 ± 28.4
	724	2.82	0.0	-71.4	-219.8	0.0	6.8	-284.3	-41.1 ± 31.3	-325.4 ± 31.3
	1024	3.16	0.0	-63.8	-219.9	0.0	6.8	-276.8	14.9 ± 37.0	-261.9 ± 37.0
k_T [10 ⁻¹⁰ m ³ mol ⁻¹ bar ⁻¹]	512	2.51	0.0	-28.9	-73.9	0.0	1.1	-101.7	1.9 ± 0.6 ^d	-99.8 ± 0.6
	724	2.82	0.0	-25.8	-73.9	0.0	1.1	-98.7	1.5 ± 0.6 ^d	-97.2 ± 0.6
	1024	3.16	0.0	-23.1	-74.0	0.0	1.1	-96.0	0.6 ± 0.8 ^d	-95.4 ± 0.8
a_p [10 ⁻⁸ m ³ mol ⁻¹ K ⁻¹]	512	2.51	0.0	2.6	9.5	0.0	0.3	12.4	13.6 ± 1.7	26.0 ± 1.7
	724	2.82	0.0	2.3	9.5	0.0	0.3	12.1	13.4 ± 2.1	25.6 ± 2.1
	1024	3.16	0.0	2.1	9.5	0.0	0.3	11.9	9.0 ± 2.4	20.8 ± 2.4
Variant B ^e										
c_p^f [J mol ⁻¹ K ⁻¹]	512	2.51	0.0	-85.5	-236.6	0.0	6.9	-315.2	-46.4 ± 28.4	-361.6 ± 28.4
	724	2.82	0.0	-76.5	-236.8	0.0	6.9	-306.4	-41.1 ± 31.3	-347.5 ± 31.3
	1024	3.16	0.0	-68.4	-236.9	0.0	6.9	-298.4	14.9 ± 37.0	-283.4 ± 37.0
k_T^g [10 ⁻¹⁰ m ³ mol ⁻¹ bar ⁻¹]	512	2.51	0.0	(-8.6)	(-23.4)	(0.0)	(0.3)	-31.6	1.9 ± 0.6 ^d	-29.7 ± 0.6
	724	2.82	0.0	(-7.7)	(-23.4)	(0.0)	(0.3)	-30.7	1.5 ± 0.6 ^d	-29.2 ± 0.6
	1024	3.16	0.0	(-6.9)	(-23.4)	(0.0)	(0.3)	-29.9	0.6 ± 0.8 ^d	-29.3 ± 0.8
a_p^f [10 ⁻⁸ m ³ mol ⁻¹ K ⁻¹]	512	2.51	0.0	3.2	11.2	0.0	0.3	14.7	13.6 ± 1.7	28.3 ± 1.7
	724	2.82	0.0	2.9	11.2	0.0	0.3	14.4	13.4 ± 2.1	27.8 ± 2.1
	1024	3.16	0.0	2.6	11.2	0.0	0.3	14.1	9.0 ± 2.4	23.0 ± 2.4

^aThe quantities reported are the parameter Y (or y) considered, the number of water molecules N_W in the system, the (average) box-edge length L , the correction terms ΔY_A , ΔY_B , ΔY_{C_1} , ΔY_{C_2} , and ΔY_D , the corresponding sum $\Delta Y_{\text{cor}}^{\square}$, the raw simulation result $\Delta Y_{\text{hyd,raw}}^{\square}$, and the corrected result $\Delta Y_{\text{hyd}}^{\square}$. Values are provided for the enthalpy H , volume V , heat capacity C_p , volume-compressibility K_T , and volume-expansivity A_p . The data refer to the standard pressure $P^\circ = 1$ bar and temperature $T^\circ = 298.15$ K. Additional details on the calculations can be found in the Supporting Information (Table S.2 and Figure S.1). Footnote c provides a comparison with previous results from ref 10 (see Supporting Information Table S2.Va therein), corresponding to the same force-field parameters, system, and calculation method IA (the small differences arise from a longer simulation time and the use of slightly different parameters for the correction scheme). ^bFor ν , c_p , k_T , and a_p , these entries refer to the quantities usually written $y_{\text{aq,raw}}^{\square}$ and y_{aq}^{\square} (equivalent to $\Delta Y_{\text{hyd,raw}}^{\square}$ and $\Delta Y_{\text{hyd}}^{\square}$ in the present context owing to eqs 8 and 9). ^cTo be compared with $y_{\text{aq,raw}}^{\square} = (9.89 \pm 2.17) \times 10^{-6}$ and $y_{\text{aq}}^{\square} = (-33.25 \pm 2.17) \times 10^{-6}$ m³ mol⁻¹ in ref 10. ^dThe corresponding values when applying a two-point forward finite difference (based on the results at 1 and 5000 bar) instead of the three-point least-squares fit are (0.7 ± 1.4) , (-1.1 ± 1.5) , and $(-2.0 \pm 1.9) \times 10^{-10}$ m³ mol⁻¹ bar⁻¹ for 512, 724, and 1024 water molecules, respectively. ^eThe entries for ΔH and ν are not repeated for variant B (identical to the corresponding entries for variant A). ^fThe individual correction terms were calculated by a centered finite difference in temperature, based on the data reported in Supporting Information Table S.2. ^gThe individual correction terms were estimated by least-squares fitting in pressure, based on the values reported in Supporting Information Table S.2, while their sum $\Delta K_{T,\text{cor}}^{\square}$ was back-calculated from $k_{T,\text{aq,raw}}^{\square}$ and $k_{T,\text{aq}}^{\square}$ (as a result, the terms may not sum up exactly to $\Delta K_{T,\text{cor}}^{\square}$ reason for which they are reported between parentheses).

are obtained if a two-point forward difference is applied for the calculation instead of the three-point least-squares fit, see footnote d in Tables 4 and 5. The trend in the raw values suggests that the residual long-range polarization of the solvent is correlated with a reduction of its volume response to pressure, presumably through a corresponding alteration of the hydrogen-bonding network. This finite-size effect is reduced by the type-B correction, leading to corrected partial molar volume-compressibilities $k_{T,\text{aq}}^{\square}$ that are similar within the statistical uncertainty (about 1×10^{-10} m³ mol⁻¹ bar⁻¹) for the three system sizes considered, evaluating to about -95×10^{-10} or $+45 \times 10^{-10}$ m³ mol⁻¹ bar⁻¹ for Na⁺ and Cl⁻, respectively, considering the largest system. As will be discussed later (section 4.2.3), however, these estimates are not considered to be accurate. The type-B correction (on the order of -20×10^{-10} to -30×10^{-10} m³ mol⁻¹ bar⁻¹) is again large for both ions but comparatively less important than for

the hydration enthalpy. Note again the important contribution of the type-C₁ correction to these estimates, of comparable magnitude (about 75×10^{-10} m³ mol⁻¹ bar⁻¹) but opposite sign for the two ions.

Finally, the raw partial molar volume-expansivities are of opposite signs for the two ions and decrease with increasing system size. This trend suggests that the residual long-range polarization of the solvent is correlated with a reduction of its volume response to temperature, presumably through a corresponding alteration of the hydrogen-bonding network. For this parameter, however, the type-B correction also decreases with increasing system size and seems unable to capture the finite-size effect appropriately. For this reason, the results obtained using 512 water molecules are considered here to be the most reliable. The corrected partial molar volume-expansivities $a_{p,\text{aq}}^{\square}$ are nevertheless similar within the statistical uncertainty (about 2×10^{-8} m³ mol⁻¹ K⁻¹) for the three

Table 5. Raw Simulation Data, Correction Terms and Corrected Results Corresponding to Hydration and Aqueous Partial Molar Parameters for Cl^- Calculated *via* Method I, along with Variants A or B^a

parameter	N_W	L [nm]	correction terms						result	
			ΔY_A	ΔY_B	ΔY_{C_1}	ΔY_{C_2}	ΔY_D	$\Delta Y_{\text{cor}}^{\square}$	$\Delta Y_{\text{hyd,raw}}^{\square}$ ^b	$\Delta Y_{\text{hyd}}^{\square}$ ^b
Variant A										
$\Delta H[\text{kJ mol}^{-1}]$	512	2.51	0.0	−79.5	82.8	0.2	0.3	3.8	$−374.0 \pm 0.9$	$−370.3 \pm 0.9$
	724	2.82	0.0	−71.1	82.9	0.2	0.3	12.2	$−379.1 \pm 1.0$	$−366.9 \pm 1.0$
	1024	3.16	0.0	−63.5	83.0	0.1	0.3	19.8	$−384.4 \pm 1.1$	$−364.6 \pm 1.1$
$\nu[10^{-6} \text{ m}^3 \text{ mol}^{-1}]$	512	2.51	0.0	−11.7	34.7	0.0	0.3	23.4	14.6 ± 0.6	38.0 ± 0.6
	724	2.82	0.0	−10.5	34.7	0.0	0.3	24.6	13.4 ± 0.6	38.0 ± 0.6
	1024	3.16	0.0	−9.4	34.8	0.0	0.3	25.7	13.4 ± 0.8^c	39.1 ± 0.8^c
$c_p[\text{J mol}^{-1} \text{ K}^{-1}]$	512	2.51	0.0	−77.9	218.5	0.2	4.5	145.3	39.1 ± 28.5	184.4 ± 28.5
	724	2.82	0.0	−70.0	218.9	0.1	4.5	153.5	26.6 ± 30.8	180.1 ± 30.8
	1024	3.16	0.0	−62.8	219.3	0.1	4.5	161.0	$−35.2 \pm 37.4$	125.8 ± 37.4
$k_T[10^{-10} \text{ m}^3 \text{ mol}^{-1} \text{ bar}^{-1}]$	512	2.51	0.0	−28.2	73.6	0.1	0.7	46.2	$−6.5 \pm 0.6^{d}$	39.6 ± 0.6
	724	2.82	0.0	−25.4	73.7	0.1	0.7	49.1	$−7.5 \pm 0.7^{d}$	41.6 ± 0.7
	1024	3.16	0.0	−22.8	73.8	0.1	0.7	51.8	$−6.8 \pm 0.8^{d}$	45.0 ± 0.8
$a_p[10^{-8} \text{ m}^3 \text{ mol}^{-1} \text{ K}^{-1}]$	512	2.51	0.0	2.5	−9.4	0.0	0.2	−6.7	$−10.5 \pm 1.7$	$−17.3 \pm 1.7$
	724	2.82	0.0	2.3	−9.4	0.0	0.2	−7.0	$−11.5 \pm 2.1$	$−18.5 \pm 2.1$
	1024	3.16	0.0	2.1	−9.5	0.0	0.2	−7.2	$−13.2 \pm 2.4$	$−20.4 \pm 2.4$
Variant B ^e										
$c_p^f[\text{J mol}^{-1} \text{ K}^{-1}]$	512	2.51	0.0	−83.5	235.4	0.2	4.6	156.7	39.1 ± 28.5	195.7 ± 28.5
	724	2.82	0.0	−75.1	235.9	0.1	4.6	165.5	26.6 ± 30.8	192.1 ± 30.8
	1024	3.16	0.0	−67.4	236.3	0.1	4.6	173.5	$−35.2 \pm 37.4$	138.3 ± 37.4
$k_T^g[10^{-10} \text{ m}^3 \text{ mol}^{-1} \text{ bar}^{-1}]$	512	2.51	0.0	(−8.4)	(23.3)	(0.0)	(0.2)	15.2	$−6.5 \pm 0.6^{d}$	8.6 ± 0.6
	724	2.82	0.0	(−7.5)	(23.3)	(0.0)	(0.2)	16.0	$−7.5 \pm 0.7^{d}$	8.5 ± 0.7
	1024	3.16	0.0	(−6.8)	(23.4)	(0.0)	(0.2)	16.8	$−6.8 \pm 0.8^{d}$	10.1 ± 0.8
$a_p^f[10^{-8} \text{ m}^3 \text{ mol}^{-1} \text{ K}^{-1}]$	512	2.51	0.0	3.1	−11.1	0.0	0.2	−7.9	$−10.5 \pm 1.7$	$−18.4 \pm 1.7$
	724	2.82	0.0	2.8	−11.2	0.0	0.2	−8.2	$−11.5 \pm 2.1$	$−19.7 \pm 2.1$
	1024	3.16	0.0	2.5	−11.2	0.0	0.2	−8.5	$−13.2 \pm 2.4$	$−21.7 \pm 2.4$

^aThe quantities reported are the parameter Y (or y) considered, the number of water molecules N_W in the system, the (average) box-edge length L , the correction terms ΔY_A , ΔY_B , ΔY_{C_1} , ΔY_{C_2} , and ΔY_D , the corresponding sum $\Delta Y_{\text{cor}}^{\square}$, the raw simulation result $\Delta Y_{\text{hyd,raw}}^{\square}$, and the corrected result $\Delta Y_{\text{hyd}}^{\square}$. Values are provided for the enthalpy H , volume V , heat capacity C_p , volume-compressibility K_T , and volume-expansivity A_p . The data refer to the standard pressure $P^\circ = 1$ bar and temperature $T^\circ = 298.15$ K. Additional details on the calculations can be found in the Supporting Information (Table S.3 and Figure S.1). Footnote c provides a comparison with previous results from Ref 10 (see Supporting Information Table S2.Va therein), corresponding to the same force-field parameters, system, and calculation method IA (the small differences arise from a longer simulation time and the use of slightly different parameters for the correction scheme). ^bFor v , c_p , k_T , and a_p , these entries refer to the quantities usually written $y_{\text{aq,raw}}^{\square}$ and y_{aq}^{\square} (equivalent to $\Delta Y_{\text{hyd,raw}}^{\square}$ and $\Delta Y_{\text{hyd}}^{\square}$ in the present context owing to eqs 8 and 9). ^cTo be compared with $v_{\text{aq,raw}}^{\square} = (14.97 \pm 2.14) \times 10^{-6}$ and $v_{\text{aq}}^{\square} = (40.65 \pm 2.14) \times 10^{-6} \text{ m}^3 \text{ mol}^{-1}$ in ref 10. ^dThe corresponding values when applying a two-point forward finite difference (based on the results at 1 and 5000 bar) instead of the three-point least-squares fit are $(−10.3 \pm 1.4)$, $(−9.2 \pm 1.6)$, and $(−11.6 \pm 1.9) \times 10^{-10} \text{ m}^3 \text{ mol}^{-1} \text{ bar}^{-1}$ for 512, 724, and 1024 water molecules, respectively. ^eThe entries for ΔH and v are not repeated for variant B (identical to the corresponding entries for variant A). ^fThe individual correction terms were calculated by a centered finite difference in temperature, based on the data reported in Supporting Information Table S.3. ^gThe individual correction terms were estimated by least-squares fitting in pressure, based on the values reported in Supporting Information Table S.3, while their sum $\Delta K_{T,\text{cor}}^{\square}$ was back-calculated from $k_{T,\text{aq,raw}}^{\square}$ and $k_{T,\text{aq}}^{\square}$ (as a result, the terms may not sum up exactly to $\Delta K_{T,\text{cor}}^{\square}$ reason for which they are reported between parentheses).

system sizes considered, evaluating to about $+26 \times 10^{-8}$ or $−17 \times 10^{-8} \text{ m}^3 \text{ mol}^{-1} \text{ K}^{-1}$ for Na^+ and Cl^- , respectively, considering the smallest system. The type-B correction (on the order of $3 \times 10^{-8} \text{ m}^3 \text{ mol}^{-1} \text{ K}^{-1}$) is again large for both ions but comparatively less important than for the hydration enthalpy. Note again the important contribution of the type- C_1 correction to these estimates, of comparable magnitude (about $9.5 \times 10^{-8} \text{ m}^3 \text{ mol}^{-1} \text{ K}^{-1}$) but opposite sign for the two ions.

4.1.2. Variant B. In terms of the hydration enthalpies and partial molar volumes, there is no distinction between variants A and B. In terms of the partial molar heat capacities, volume-expansivities, and volume-compressibilities, the raw values are also identical in the two variants.

Considering the values obtained using 512 water molecules to be the most reliable (section 4.1.1), the corrected partial molar heat capacities $c_{p,\text{aq}}^{\square}$ calculated using variant B, evaluating

to about $−362$ or $+196 \text{ J mol}^{-1} \text{ K}^{-1}$ for Na^+ and Cl^- , respectively, differ noticeably from those calculated using variant A (about $−339$ or $+184 \text{ J mol}^{-1} \text{ K}^{-1}$, respectively). The difference is due to larger magnitudes of the type-B and type- C_1 correction terms, mainly related to the nonlinear dependence of the density of water on temperature. Considering the very large statistical uncertainty (about $30 \text{ J mol}^{-1} \text{ K}^{-1}$) affecting the results, the discrepancy between the two variants remains nevertheless acceptable.

The corrected partial molar volume-compressibilities $k_{T,\text{aq}}^{\square}$ calculated using variant B are similar within the statistical uncertainty for the three system sizes considered, evaluating to about $−29 \times 10^{-10}$ or $+10 \times 10^{-10} \text{ m}^3 \text{ mol}^{-1} \text{ bar}^{-1}$ for Na^+ and Cl^- , respectively, considering the largest system. These values differ considerably from those obtained using variant A (about $−95 \times 10^{-10}$ or $+45 \times 10^{-10} \text{ m}^3 \text{ mol}^{-1} \text{ bar}^{-1}$, respectively). Here, the difference is due to much smaller magnitudes of the

Table 6. Raw Simulation Data, Correction Terms and Corrected Results Corresponding to Hydration and Aqueous Partial Molar Parameters for Na⁺ Calculated *via* Method II, along with Variants A or B^a

parameter	N_W	L [nm]	correction terms						result		
			ΔY_A	ΔY_B	ΔY_{C_1}	ΔY_{C_2}	ΔY_D	$\Delta Y_{\text{cor}}^{\square}$	ΔY_{cav}	$\Delta Y_{\text{chg,raw}}$	$\Delta Y_{\text{hyd}}^{\square\text{ }b}$
Variant A											
ΔG [kJ mol ⁻¹]	724	2.82	0.0	-68.5	-77.2	0.0	-0.9	-146.6	10.5 ± 0.2	-295.0 ± 0.7	-431.2 ± 0.7
	1024	3.16	0.0	-61.1	-77.2	0.0	-0.9	-139.2 ^c	11.7 ± 0.2 ^d	-303.4 ± 0.6 ^e	-430.9 ± 0.6
ΔH [kJ mol ⁻¹]	724	2.82	0.0	-71.6	-83.1	0.0	0.4	-154.3	5.7 ± 1.4	-314.4 ± 5.3	-463.0 ± 5.5
	1024	3.16	0.0	-63.9	-83.1	0.0	0.4	-146.6 ^f	7.5 ± 1.4 ^g	-333.2 ± 5.2 ^h	-472.3 ± 5.4
s [J mol ⁻¹ K ⁻¹]	724	2.82	0.0	-10.4	-19.8	-0.1	4.5	-25.8	-15.8 ± 4.8	-65.0 ± 17.5	-106.6 ± 18.1
	1024	3.16	0.0	-9.3	-19.8	-0.1	4.5	-24.7 ⁱ	-14.3 ± 4.8 ^j	-100.0 ± 17.3 ^k	-139.1 ± 18.0
ν [10 ⁻⁶ m ³ mol ⁻¹]	1024	3.16	0.0	-9.6	-34.9	0.0	0.4	-44.0	13.9 ± 0.3	0.6 ± 0.8	-29.5 ± 0.9
Variant B ^l											
ΔH^m [kJ mol ⁻¹]	724	2.82	0.0	(-71.5)	(-82.7)	(0.0)	(0.4)	-153.8	5.7 ± 1.4	-314.4 ± 5.3	-462.4 ± 5.5
	1024	3.16	0.0	(-63.8)	(-82.7)	(0.0)	(0.4)	-146.1	7.5 ± 1.4 ^g	-333.2 ± 5.2 ^h	-471.8 ± 5.4
s^m [J mol ⁻¹ K ⁻¹]	724	2.82	0.0	(-10.0)	(-18.5)	(-0.1)	(4.5)	-24.1	-15.8 ± 4.8	-65.0 ± 17.5	-104.9 ± 18.1
	1024	3.16	0.0	(-9.0)	(-18.5)	(-0.1)	(4.5)	-23.0	-14.3 ± 4.8 ^j	-100.0 ± 17.3 ^k	-137.4 ± 18.0
ν^m [10 ⁻⁶ m ³ mol ⁻¹]	1024	3.16	0.0	(-4.8)	(-18.7)	(0.0)	(0.2)	-23.2	13.9 ± 0.3	0.6 ± 0.8	-8.7 ± 0.9

^aThe quantities reported are the parameter Y (or y) considered, the number of water molecules N_W in the system, the (average) box-edge length L , the correction terms ΔY_A , ΔY_B , ΔY_{C_1} , ΔY_{C_2} , and ΔY_D , the corresponding sum $\Delta Y_{\text{cor}}^{\square}$, the cavitation term ΔY_{cav} , the raw charging term $\Delta Y_{\text{chg,raw}}$, and the corrected result $\Delta Y_{\text{hyd}}^{\square}$. Values are provided for the free energy G , enthalpy H , entropy S , and volume V . The data refer to the standard pressure $P^\circ = 1$ bar and temperature $T^\circ = 298.15$ K. Additional details on the calculations can be found in the Supporting Information (Table S.4 and Figure S.2). Footnotes c–k provide a comparison with previous results from refs 10 (see Supporting Information Table S2.IVa therein) and ref 19 (see Table S.7 therein) corresponding to the same force-field parameters, system, and calculation method IIA (the small differences arise from a longer simulation time and the use of slightly different parameters for the correction scheme). ^bFor s and ν , this entry refers to the quantity usually written y_{aq}^{\square} (equivalent to $\Delta Y_{\text{hyd}}^{\square}$ in the present context owing to eqs 8 and 9). ^cTo be compared with -138.65 kJ mol⁻¹ in ref 10. ^dTo be compared with 12.49 ± 0.27 kJ mol⁻¹ in ref 10. ^eTo be compared with -302.20 ± 0.64 kJ mol⁻¹ in ref 10. ^fTo be compared with -161.9 kJ mol⁻¹ based on refs 10 and 19 using the Gibbs equation. ^gTo be compared with 8.45 ± 3.81 kJ mol⁻¹ based on refs 10 and 19 using the Gibbs equation. ^hTo be compared with -327.33 ± 7.77 kJ mol⁻¹ based on refs 10 and 19 using the Gibbs equation. ⁱTo be compared with -78.12 J mol⁻¹ K⁻¹ in ref 19 (the large difference arises from the use of a different value of $\partial_T \rho'$ in the two studies). ^jTo be compared with -13.25 ± 12.75 J mol⁻¹ K⁻¹ in ref 19. ^kTo be compared with -80.93 ± 25.98 J mol⁻¹ K⁻¹ in ref 19. ^lThe entry for ΔG is not repeated for variant B (identical to the corresponding entry for variant A). ^mThe individual correction terms were estimated by least-squares fitting in temperature or pressure, based on the values reported in Supporting Information Table S.4, while their sum $\Delta Y_{\text{cor}}^{\square}$ was back-calculated from $\Delta Y_{\text{hyd,raw}}^{\square}$ (as obtained by variant A) and $\Delta Y_{\text{hyd}}^{\square}$ (as a result, the terms may not sum up exactly to $\Delta Y_{\text{cor}}^{\square}$, reason for which they are reported between parentheses).

type-B and type-C₁ correction terms, mainly related to the nonlinear dependence of the density of water on pressure. The effect of this nonlinearity is clearly visible in panels c and d of Figure S.1 in the Supporting Information, which shows that the corrected values of $\nu_{\text{aq}}^{\square}$ at the three pressures considered are not aligned. As a result, the calculated values are quite sensitive to the calculation procedure. As will be discussed later (section 4.2.3), these estimates are considered to be more accurate than those of method IA.

The corrected partial molar volume-expansivities $a_{P,\text{aq}}^{\square}$ calculated using variant B also decrease slightly with increasing system size but are nevertheless similar within the statistical uncertainty for the three system sizes considered, evaluating to about $+28 \times 10^{-8}$ or -18×10^{-8} m³ mol⁻¹ K⁻¹ for Na⁺ and Cl⁻, respectively, considering the values obtained using 512 water molecules to be the most reliable (section 4.1.1). These values are in excellent agreement with those obtained using variant A (about $+26 \times 10^{-8}$ or -17×10^{-8} m³ mol⁻¹ K⁻¹, respectively), considering the same system size.

4.2. Method II. The $\Delta G_{\text{hyd}}^{\square}$, $\Delta H_{\text{hyd}}^{\square}$, s_{aq}^{\square} , and $\nu_{\text{aq}}^{\square}$ estimates obtained using method II (sections 2.3.2 and 3.3) considering two different system sizes (724 or 1024 water molecules; only 1024 for $\nu_{\text{aq}}^{\square}$) for the Na⁺ or Cl⁻ ions are reported in Tables 6 and 7, respectively. More details on the calculations can also be found in Tables S.4 and S.5 as well as Figure S.2 of the Supporting Information document. The results for variants A (section 2.4.1) and B (section 2.4.2) are discussed separately in the two following sections.

4.2.1. Variant A. For both Na⁺ and Cl⁻, the raw hydration free energy is negative and increases in magnitude with increasing system size, which indicates that the systems considered fail to encompass a sufficient volume of correctly polarized solvent around the ion. For Na⁺, this finite-size effect is appropriately compensated by the type-B correction, leading to a corrected hydration free energy $\Delta G_{\text{hyd}}^{\square}$ of about -431 kJ mol⁻¹. For Cl⁻, the finite-size effect is slightly overcompensated, leading to a corrected hydration free energy that slightly decreases in magnitude with increasing system size, evaluating to about -318 kJ mol⁻¹ for the largest system. These values can be compared to the values of -428.4 ± 0.8 or -318.1 ± 1.1 for Na⁺ and Cl⁻, respectively, obtained previously¹⁰ with the same force-field parameters, system (1024 water molecules), and calculation method. The small difference for Na⁺ arises from a longer simulation time and the use of slightly different parameters for the cavitation free energy calculation (different set of λ points) and for the correction scheme. In both cases, the type-B correction for finite-size effects (on the order of -60 to -70 kJ mol⁻¹) is very large for the truly microscopic system sizes considered, which remain very far from a bulk (infinite-dilution) situation. The cavitation contribution (about 10 – 15 kJ mol⁻¹) is small compared to the charging term. Note also the important contribution of the type-C₁ correction term for improper potential summation to these estimates, of comparable magnitude (about 77 kJ mol⁻¹) but opposite sign for the two ions.

For the hydration enthalpy, similar observations hold as those made in the context of method I (section 4.1). However,

Table 7. Raw Simulation Data, Correction Terms, and Corrected Results Corresponding to Hydration and Aqueous Partial Molar Parameters for Cl^- Calculated *via* Method II, along with Variants A or B^a

parameter	N_W	L [nm]	correction terms						result		
			ΔY_A	ΔY_B	ΔY_{C_1}	ΔY_{C_2}	ΔY_D	$\Delta Y_{\text{cor}}^{\square}$	ΔY_{cav}	$\Delta Y_{\text{chg,raw}}$	$\Delta Y_{\text{hyd}}^{\square b}$
Variant A											
ΔG [kJ mol ⁻¹]	724	2.82	0.0	-68.1	77.0	0.1	-0.6	8.4	11.0 ± 0.3	-340.8 ± 0.6	-321.4 ± 0.7
	1024	3.16	0.0	-60.8	77.1	0.1	-0.6	15.7 ^c	13.8 ± 0.3 ^d	-347.9 ± 0.6 ^e	-318.4 ± 0.7
ΔH [kJ mol ⁻¹]	724	2.82	0.0	-71.1	82.9	0.2	0.3	12.2	-1.9 ± 2.5	-363.6 ± 4.6	-353.2 ± 5.2
	1024	3.16	0.0	-63.5	83.0	0.1	0.3	19.8 ^f	4.4 ± 2.5 ^g	-374.2 ± 4.8 ^h	-350.0 ± 5.5
s [J mol ⁻¹ K ⁻¹]	724	2.82	0.0	-10.2	19.7	0.3	3.0	12.8	-43.2 ± 8.3	-76.3 ± 15.3	-106.8 ± 17.4
	1024	3.16	0.0	-9.2	19.7	0.2	3.0	13.8 ⁱ	-31.6 ± 8.4 ^j	-88.2 ± 16.1 ^k	-106.1 ± 18.2
ν [10 ⁻⁶ m ³ mol ⁻¹]	1024	3.16	0.0	-9.4	34.8	0.0	0.3	25.7	36.1 ± 0.6	-19.1 ± 0.8	42.7 ± 1.0
Variant B ^l											
ΔH^m [kJ mol ⁻¹]	724	2.82	0.0	(-71.0)	(82.5)	(0.2)	(0.3)	11.9	-1.9 ± 2.5	-363.6 ± 4.6	-353.5 ± 5.2
	1024	3.16	0.0	(-63.4)	(82.6)	(0.1)	(0.3)	19.5	4.4 ± 2.5 ^g	-374.2 ± 4.8 ^h	-350.3 ± 5.5
s^m [J mol ⁻¹ K ⁻¹]	724	2.82	0.0	(-9.8)	(18.3)	(0.3)	(3.0)	11.8	-43.2 ± 8.3	-76.3 ± 15.3	-107.7 ± 17.4
	1024	3.16	0.0	(-8.8)	(18.4)	(0.2)	(3.0)	12.8	-31.6 ± 8.4 ^j	-88.2 ± 16.1 ^k	-107.1 ± 18.2
ν^m [10 ⁻⁶ m ³ mol ⁻¹]	1024	3.16	0.0	(-4.7)	(18.6)	(0.0)	(0.1)	14.1	36.1 ± 0.6	-19.1 ± 0.8	31.1 ± 1.0

^aThe quantities reported are the parameter Y (or y) considered, the number of water molecules N_W in the system, the (average) box-edge length L , the correction terms ΔY_A , ΔY_B , ΔY_{C_1} , ΔY_{C_2} , and ΔY_D , the corresponding sum $\Delta Y_{\text{cor}}^{\square}$, the cavitation term ΔY_{cav} , the raw charging term $\Delta Y_{\text{chg,raw}}$, and the corrected result $\Delta Y_{\text{hyd}}^{\square}$. Values are provided for the free energy G , enthalpy H , entropy S , and volume V . The data refer to the standard pressure $P^\circ = 1$ bar and temperature $T^\circ = 298.15$ K. Additional details on the calculations can be found in the Supporting Information (Table S.5 and Figure S.2). Footnotes c–k provide a comparison with previous results from ref 10 (see Supporting Information Table S2.IVa therein) and ref 19 (see Table S.7 therein) corresponding to the same force-field parameters, system, and calculation method IIA (the small differences arise from a longer simulation time and the use of slightly different parameters for the correction scheme). ^bFor s and v , this entry refers to the quantity usually written y_{aq}^{\square} (equivalent to $\Delta Y_{\text{hyd}}^{\square}$ in the present context owing to eqs 8 and 9). ^cTo be compared with 15.34 kJ mol⁻¹ in ref 10. ^dTo be compared with 14.97 ± 0.46 kJ mol⁻¹ in ref 10. ^eTo be compared with -348.39 ± 0.61 kJ mol⁻¹ in ref 10. ^fTo be compared with 26.3 kJ mol⁻¹ based on refs 10 and 19 using the Gibbs equation. ^gTo be compared with 6.41 ± 7.10 kJ mol⁻¹ based on refs 10 and 19 using the Gibbs equation. ^hTo be compared with -381.77 ± 7.90 kJ mol⁻¹ based on refs 10 and 19 using the Gibbs equation. ⁱTo be compared with 36.86 J mol⁻¹ K⁻¹ in ref 19 (the large difference arises from the use of a different value of $\partial_T \rho'$ in the two studies). ^jTo be compared with -27.75 ± 23.75 J mol⁻¹ K⁻¹ in ref 19. ^kTo be compared with -114.43 ± 26.40 J mol⁻¹ K⁻¹ in ref 19. ^lThe entry for ΔG is not repeated for variant B (identical to the corresponding entry for variant A). ^mThe individual correction terms were estimated by least-squares fitting in temperature or pressure, based on the values reported in Supporting Information Table S.5, while their sum $\Delta Y_{\text{cor}}^{\square}$ was back-calculated from $\Delta Y_{\text{hyd,raw}}^{\square}$ (as obtained by variant A) and $\Delta Y_{\text{hyd}}^{\square}$ (as a result, the terms may not sum up exactly to $\Delta Y_{\text{cor}}^{\square}$, the reason for which they are reported between parentheses).

here, the system-size dependence of the raw values appears to be slightly more pronounced for both ions. The corrected results present a larger residual system-size dependence for Na^+ compared to Cl^- , and this residual dependence for Na^+ corresponds to a more negative solvation enthalpy in the largest system. In spite of these small differences, the corrected hydration enthalpies $\Delta H_{\text{hyd}}^{\square}$ calculated using method II, evaluating to about -472 or -350 kJ mol⁻¹ for Na^+ and Cl^- , respectively, considering the largest system, are in acceptable agreement with those obtained using method I (about -476 or -365 kJ mol⁻¹, respectively), noting that these values are affected by larger statistical uncertainties (about 6 kJ mol⁻¹). Here also, the cavitation contribution is very small compared to the charging term.

The charging component of the raw partial molar entropies is negative for the two ions and increases in magnitude with increasing system size. This trend is easily understood considering that the residual long-range polarization of the solvent is correlated with an intrinsic ordering of the solvent molecules. The corresponding cavitation component is also negative for the two ions. For Na^+ , it is relatively small and system-size independent. For Cl^- , it is significantly larger and decreases in magnitude with increasing system size. After application of the correction terms, and considering the largest system for Na^+ , the corrected partial molar entropies s_{aq}^{\square} evaluate to about -139 or -106 J mol⁻¹ K⁻¹ for Na^+ and Cl^- , respectively, with relatively large statistical uncertainties (about 18 J mol⁻¹ K⁻¹). Observing that the error on $\Delta H_{\text{hyd}}^{\square}$ is

lower in method I than in method II, possibly more accurate estimates for s_{aq}^{\square} can be deduced from the hydration free energies (about -431 or -318 kJ mol⁻¹, respectively) along with the hydration enthalpies of method I (about -476 or -365 kJ mol⁻¹, respectively) using the Gibbs equation, resulting in about -153 or -155 J mol⁻¹ K⁻¹ for Na^+ and Cl^- , respectively. For the two ions, the type-B correction term (on the order of -10 J mol⁻¹ K⁻¹), the type-C₁ correction term (magnitude on the order of 20 J mol⁻¹ K⁻¹), and the cavitation term (on the order of -15 or -80 J mol⁻¹ K⁻¹ for Na^+ and Cl^- , respectively) all provide contributions of large magnitudes. In practice, the accurate calculation of ionic solvation entropies is notoriously difficult,^{16–21} and the results also turn out to be very sensitive to the detailed structural properties of the employed water model, as well as its ability to reproduce the experimental temperature dependence of the density and permittivity (see e.g. Table S.7 in ref 19).

For the partial molar volume, only one system size was considered. For this parameter, the cavitation component, accounting for the excluded-volume of the ion, is expectedly positive and becomes the leading term. For Na^+ , the charging component, accounting for electrostrictive effects, is negligible. In contrast, for Cl^- , this term is important and expectedly negative. The corrected partial molar volumes v_{aq}^{\square} calculated using method II, evaluating to about -30 × 10⁻⁶ or +43 × 10⁻⁶ m³ mol⁻¹ for Na^+ and Cl^- , respectively, are in good agreement with those obtained using method I (about -33 × 10⁻⁶ or

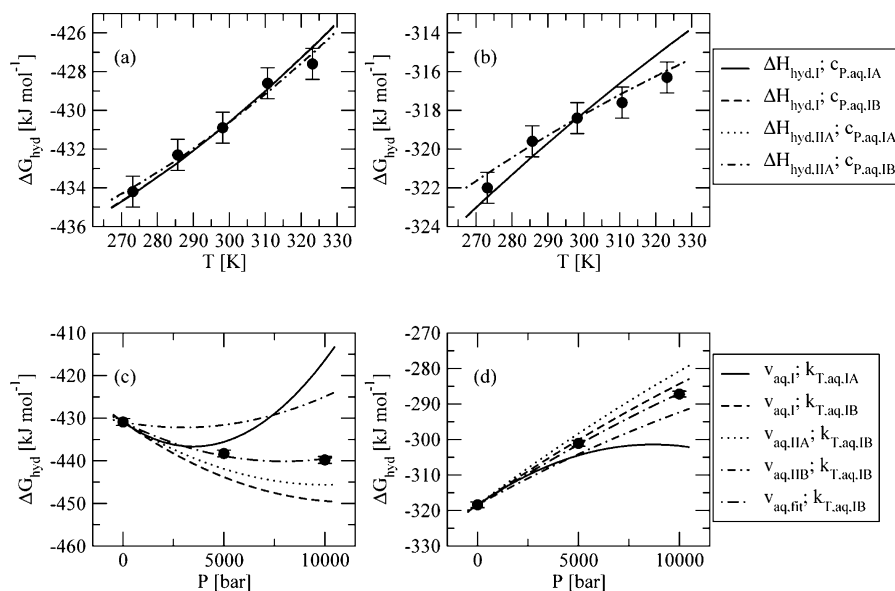


Figure 1. Assessment of the aqueous partial molar heat capacities and volume-compressibilities calculated for Na^+ or Cl^- *via* methods IA or IB against the pressure or temperature dependence of hydration free energies calculated *via* method II. The top panels (a,b) show the temperature dependence at $P = P^\circ$ and the bottom panels (c,d) the pressure dependence at $T = T^-$ of the corrected hydration free energy ΔG_{hyd} . The left panels (a,c) refer to Na^+ and the right panels (b,d) to Cl^- . The system considered is the one involving 1024 water molecules. Curves corresponding to the model functions of eq 49 for the temperature dependence and eq 50 for the pressure dependence, along with various combinations of parameters, are also displayed. For panels a and b, the different curves rely on $\Delta G_{\text{hyd}}^\square$ from method II, $\Delta H_{\text{hyd}}^\square$ from either method I ($\Delta H_{\text{hyd,I}}^\square$) or method IIA ($\Delta H_{\text{hyd,IIA}}^\square$), the latter essentially identical to IIB, and $c_{\text{P,aq}}^\square$ from either method IA ($c_{\text{P,aq,IA}}^\square$) or method IB ($c_{\text{P,aq,IB}}^\square$). Note that the effect of $c_{\text{P,aq}}^\square$ is very small, so that the corresponding curves are essentially indistinguishable. For panels c and d, the different curves rely on $\Delta G_{\text{hyd}}^\square$ from method II, v_{aq}^\square from either method I ($v_{\text{aq,I}}^\square$), method IIA ($v_{\text{aq,IIA}}^\square$), or method IIB ($v_{\text{aq,IIB}}^\square$), and $k_{\text{T,aq}}^\square$ from either method IA ($k_{\text{T,aq,IA}}^\square$) or method IB ($k_{\text{T,aq,IB}}^\square$). An additional curve corresponds to $k_{\text{T,aq,IB}}^\square$ along with $v_{\text{aq,fit}}^\square$ values leading to the best fit of the model equation to the hydration free energy. These values are $v_{\text{aq,fit}}^\square = -23.3 \times 10^{-6}$ or $+36.4 \times 10^{-6} \text{ m}^3 \text{ mol}^{-1}$ for Na^+ and Cl^- , respectively.

$+39 \times 10^{-6} \text{ m}^3 \text{ mol}^{-1}$, respectively), the values being affected by similar statistical uncertainties (about $1 \times 10^{-6} \text{ m}^3 \text{ mol}^{-1}$).

4.2.2. Variant B. In terms of the hydration free energy, there is no distinction between variants A and B. In terms of the hydration enthalpy as well as the partial molar volume and entropy, the raw values are also identical in the two variants.

The corrected hydration enthalpies $\Delta H_{\text{hyd}}^\square$ and partial molar entropies s_{aq}^\square calculated using variant B are very close to the corresponding values calculated using variant A, with maximal differences on the order of 1 kJ mol^{-1} and $2 \text{ J mol}^{-1} \text{ K}^{-1}$, respectively.

In contrast, the corrected partial molar volumes v_{aq}^\square calculated using variant B, evaluating to about -9×10^{-6} or $+31 \times 10^{-6} \text{ m}^3 \text{ mol}^{-1}$ for Na^+ and Cl^- , respectively, differ significantly from those obtained using variant A (about -30×10^{-6} or $+43 \times 10^{-6} \text{ m}^3 \text{ mol}^{-1}$, respectively) or using method I (about -33×10^{-6} or $+39 \times 10^{-6} \text{ m}^3 \text{ mol}^{-1}$, respectively), the values being affected by similar statistical uncertainties (about $1 \times 10^{-6} \text{ m}^3 \text{ mol}^{-1}$). The difference is mainly due to smaller magnitudes of the type- C_1 correction term, related to the nonlinear dependence of the density of water on pressure. For Na^+ , for which the difference is most pronounced, the effect of this nonlinearity is clearly visible in panel c of Figure S.2 in the Supporting Information, which shows that the corrected values of the charging component of $\Delta G_{\text{hyd}}^\square$ at the three pressures considered are not aligned. As a result, the calculated values are quite sensitive to the calculation procedure.

4.2.3. Second-Order Derivatives. The evaluation of the hydration free energy as a function of pressure or/and temperature could not be performed with sufficient accuracy to permit a reliable determination of the second-order

derivatives $c_{\text{P,aq}}^\square$, $k_{\text{T,aq}}^\square$ and $a_{\text{P,aq}}^\square$ *via* method II. This is clear from the free-energy curves displayed in Figure S.2 in the Supporting Information, which suggest that obtaining accurate curvature information is essentially impossible. However, given the important differences in the estimates of $k_{\text{T,aq}}^\square$ and, to a lesser extent, $c_{\text{P,aq}}^\square$ *via* the two variants of method I (section 4.1.2), these estimates were checked for compatibility with the curvature of the solvation free-energy curves as a function of pressure or/and temperature, given the associated uncertainty. This comparison is performed in Figure 1, based on the model functions

$$\Delta G_{\text{hyd}}(T) = \Delta H_{\text{hyd}}^\square + c_{\text{P,aq}}^\square(T - T^-) - T \left(\frac{\Delta H_{\text{hyd}}^\square - \Delta G_{\text{hyd}}^\square}{T^-} + c_{\text{P,aq}}^\square \ln \frac{T}{T^-} \right) \quad (49)$$

for the temperature dependence of ΔG_{hyd} at $P = P^\circ$ and

$$\Delta G_{\text{hyd}}(P) = \Delta G_{\text{hyd}}^\square + v_{\text{aq}}^\square(P - P^\circ) - (1/2)k_{\text{T,aq}}^\square(P - P^\circ)^2 \quad (50)$$

for the pressure dependence of ΔG_{hyd} at $T = T^-$. These are the appropriate thermodynamic equations for an extrapolation of ΔG_{hyd} assuming a temperature-independent $c_{\text{P,aq}}$ (equal to $c_{\text{P,aq}}^\square$) and a pressure-independent $k_{\text{T,aq}}$ (equal to $k_{\text{T,aq}}^\square$). Although a combined equation for the simultaneous pressure and temperature dependence, also assuming a constant $a_{\text{P,aq}}$ (equal to $a_{\text{P,aq}}^\square$), could easily be derived as well, this comparison was left out considering that the $a_{\text{P,aq}}^\square$ estimates obtained using the two variants of method I are in good agreement (section 4.1.2).

Table 8. Corrected Results Corresponding to Hydration and Aqueous Partial Molar Parameters for Na⁺ and Cl[−], Considered by the Authors of This Article As the Most Reliable Estimates Based on the Present Simulations^a

property $\Delta Y_{\text{hyd}}^{\square}$ ^b	sel.	Na ⁺		Cl [−]		Na ⁺ + Cl [−]		H ⁺		
		sim.	rec.	sim.	rec.	sim.	exptl.	sim. (Na ⁺) ^c	sim. (Cl [−]) ^d	rec.
ΔG [kJ mol ^{−1}]	II	−430.9	−427.41	−318.4	−316.55	−749.3	−743.96	−1111.4	−1106.1	−1107.95
ΔH [kJ mol ^{−1}]	I	−476.3	−450.20	−364.6	−328.8	−840.9	−779.0	−1162.9	−1101.0	−1136.75
s [J mol ^{−1} K ^{−1}]	I+II ^e	−152.5	−76.40	−154.8	−41.09	−307.3	−117.49	−172.7	17.1	−96.62
v [10 ^{−6} m ³ mol ^{−1}]	IIA	−29.5	−5.86	42.7	22.21	13.2	16.35	−28.2	−25.0	−4.5
c_p [J mol ^{−1} K ^{−1}]	IA ^f	−339.0	−43.84	184.4	−81.90	−154.6	−125.74	−381.0	−352.1	−85.87
k_T^g [10 ^{−10} m ³ mol ^{−1} bar ^{−1}]	IB	−29.3	−27.45	10.1	−21.29	−19.2	−48.74	13.1	−16.4	15.0
a_p [10 ^{−8} m ³ mol ^{−1} K ^{−1}]	IA ^f	26.0	2.42	−17.3	4.62	8.8	7.04	20.6	18.9	−3.0

^aThe selection was made based on the discussion presented in sections 4.1 and 4.2, and the selected (sel.) calculation method (method I or II), variant (variant A or B), and system size (by default, system with 1024 water molecules) are indicated. A detailed summary of the calculation results for the four combinations of methods and variants, and for all considered system sizes, can also be found in Tables S.6–S.8 of the Supporting Information. The quantities reported are the parameter Y (or y) considered and the corrected simulation estimate $\Delta Y_{\text{hyd}}^{\square}$. Values are provided for the free energy G , enthalpy H , entropy S , volume V , heat capacity C_p , volume-compressibility K_T , and volume-expansivity A_p . The reported values for Na⁺ + Cl[−] correspond to sum of parameters over the individual ions Na⁺ and Cl[−]. The data refer to the standard pressure $P^\circ = 1$ bar and temperature $T^\circ = 298.15$ K. The simulation values are reported from the corresponding entries of Tables 4–7. The simulation (sim.) results are compared with recommended (rec.) or experimental (exptl.) values, taken from the corresponding entry in Table 2. For the individual ions, the recommended values are inferred from experimental results but correspond to experimentally elusive quantities and are thus to be considered with some caution.¹¹ For the ion pair, the experimental values are in principle experimentally accessible. However, the entries for $c_{p,\text{aq}}^{\square}$, $k_{T,\text{aq}}^{\square}$, and $a_{p,\text{aq}}^{\square}$ should still be taken with some caution in view of the sparseness and indirect nature of the corresponding experimental determinations.¹¹ Values for the proton inferred from the simulations are also provided and compared to corresponding recommended data. ^bFor s , v , c_p , k_T , and a_p , the entries of this table refer to the quantities usually written y_{aq}^{\square} (equivalent to $\Delta Y_{\text{hyd}}^{\square}$ in the present context owing to eqs 8 and 9). ^cValue for the proton deduced from the simulation results for Na⁺ as $\Delta Y_{\text{hyd},\text{sim}}^{\square}[\text{Na}^+] - \Delta Y_{\text{hyd},\text{rec}}^{\square}[\text{Na}^+] + \Delta Y_{\text{hyd},\text{rec}}^{\square}[\text{H}^+]$, “rec” indicating the recommended value of Table 2 and “sim” the value from the simulation. ^dValue for the proton deduced from the simulation results for Cl[−] as $-\Delta Y_{\text{hyd},\text{sim}}^{\square}[\text{Cl}^-] + \Delta Y_{\text{hyd},\text{rec}}^{\square}[\text{Cl}^-] + \Delta Y_{\text{hyd},\text{rec}}^{\square}[\text{H}^+]$, “rec” indicating the recommended value of Table 2 and “sim” the value from the simulation. ^eValue calculated on the basis of the Gibbs equation using ΔH from method I and ΔG from method II. ^fSystem with 512 water molecules. ^gValue supported by compatibility analysis.

Considering the temperature dependence of the hydration free energy for Na⁺, all combinations of $\Delta H_{\text{hyd}}^{\square}$ (I or IIA, the latter essentially equal to IIB) and $c_{p,\text{aq}}^{\square}$ (IA and IB) estimates are compatible with the ΔG_{hyd} curve, given the associated uncertainty. For the Cl[−] ion, the model function obtained using the $\Delta H_{\text{hyd}}^{\square}$ estimate from method IIA (essentially equal to IIB) is clearly more accurate than that obtained using the corresponding estimate from method I, the effect of the selected $c_{p,\text{aq}}^{\square}$ (IA and IB) estimate being negligible. These observations illustrate that the slope of the ΔG_{hyd} curve provides sufficient information on $\Delta H_{\text{hyd}}^{\square}$ (similar values from I and IIA for Na⁺, larger difference for Cl[−]), but that the corresponding curvature is too small to provide reliable information on $c_{p,\text{aq}}^{\square}$, given the uncertainty affecting the data.

Considering the pressure dependence of the hydration free energy for both ions, the model functions obtained using the $k_{T,\text{aq}}^{\square}$ estimates from method IA clearly evidence too pronounced curvatures. Using the $k_{T,\text{aq}}^{\square}$ estimates from method IB, the curve relying on the v_{aq}^{\square} estimate from method IIA is the most accurate for Na⁺, and that relying on the v_{aq}^{\square} estimate from method I is the most accurate for Cl[−]. Reoptimizing v_{aq}^{\square} for best agreement results in values of about -23×10^{-6} or $+36 \times 10^{-6}$ m³ mol^{−1} for Na⁺ and Cl[−], respectively, acceptably close to the values for method IIA (-30×10^{-6} or $+43 \times 10^{-6}$ m³ mol^{−1}, respectively). Following from this analysis, the v_{aq}^{\square} estimates from method IIA and the $k_{T,\text{aq}}^{\square}$ estimates from method IB were retained as the most reliable.

4.3. Comparison with Available Experimental Data. A detailed summary of the calculation results for the four combinations of methods and variants, and for all considered system sizes, is provided in Tables S.6–S.8 of the Supporting Information document. On the basis of the discussion of sections 4.1 and 4.2, values considered by the authors of this article as the most reliable were selected for each parameter and

for both ions. These values are reported in Table 8 and compared with available experimental or recommended data, the latter based on or derived from the numbers reported in Table 2.

For the Na⁺ and Cl[−] ions taken individually, the comparison between the calculated numbers and the recommended values from Table 2 should be performed with caution, considering that the latter estimates depend on a specific choice for the experimentally elusive¹¹ proton parameters $\Delta G_{\text{hyd}}^{\square}[\text{H}^+]$, $\Delta H_{\text{hyd}}^{\square}[\text{H}^+]$, $s_{\text{aq}}^{\square}[\text{H}^+]$, $v_{\text{aq}}^{\square}[\text{H}^+]$, $c_{p,\text{aq}}^{\square}[\text{H}^+]$, $k_{T,\text{aq}}^{\square}[\text{H}^+]$, and $a_{p,\text{aq}}^{\square}[\text{H}^+]$. For both ions, the calculated and recommended hydration free energies are in excellent agreement. This is no surprise considering that the ion–solvent Lennard-Jones interaction parameters used here were explicitly calibrated against these recommended values¹⁰ (set L, assuming $\Delta G_{\text{hyd}}^{\square}[\text{H}^+] = -1100$ kJ mol^{−1} or, equivalently, $\Delta G_{\text{hyd}}^{\square}[\text{H}^+] = -1107.95$ kJ mol^{−1}). For all of the other parameters, the agreement is qualitative at best, which may result either from inaccuracies in the computational model and calculation procedure, from inappropriate values for the recommended parameters of the proton, or from a combination of both. For $\Delta H_{\text{hyd}}^{\square}$, qualitative agreement is achieved, i.e., the calculated and recommended values have the same orders of magnitudes for the two ions. For s_{aq}^{\square} , the two ions are characterized by large negative values, the calculated ones being considerably larger in magnitude. For v_{aq}^{\square} , the two ions are characterized by values of opposite signs. Na⁺ has a negative partial molar volume, suggesting a dominance of electrostrictive over excluded-volume effects, the opposite being true for Cl[−]. For $c_{p,\text{aq}}^{\square}$, $k_{T,\text{aq}}^{\square}$, and $a_{p,\text{aq}}^{\square}$, the calculated and recommended values are of the same sign for Na⁺ but of opposite signs for Cl[−]. For $c_{p,\text{aq}}^{\square}$ and $a_{p,\text{aq}}^{\square}$, the calculated values are also considerably larger in magnitude, whereas the orders of magnitude are comparable for $k_{T,\text{aq}}^{\square}$.

In contrast to the single-ion parameters, the sums of these parameters for the $\text{Na}^+ + \text{Cl}^-$ pair are in principle experimentally accessible, and are thus referred to here as experimental rather than recommended. Note, however, that for the second-derivative quantities $c_{p,\text{aq}}^\square$, $k_{T,\text{aq}}^\square$, and $a_{p,\text{aq}}^\square$, the experimental estimates even for these sums are not highly reliable, in view of the very small number of independent determinations and of the limited consistency among the resulting estimates.¹¹ Expectedly, the calculated and experimental ion-pair hydration free energies are in excellent agreement. On the other hand, the enthalpy–entropy partitioning is not accurate, both $\Delta H_{\text{hyd}}^\square$ and s_{aq}^\square being overestimated in magnitude in the present calculations. This failure is likely due at least in part to the use of an implicit-polarization model for the ion–water interactions, which has already been suggested to result in an overstructuring of the hydration shells.^{65–67} Note, however, that other authors report comparable ion–water radial distribution functions for implicit- and explicit-polarization models, while density functional calculations employing a plane-wave basis set resulted in less structured hydration shells.⁶⁸ As observed previously,¹⁰ the calculated ion-pair partial molar volume v_{aq}^\square is in good agreement with the corresponding experimental estimate, although the partitioning in terms of single-ion volumes differs significantly from that suggested by the recommended value $v_{\text{aq}}^\square[\text{H}^+] = -4.5 \times 10^{-6} \text{ m}^3 \text{ mol}^{-1}$. A similar observation applies to the partitioning of the partial molar heat capacity, for which the calculated ion-pair $c_{p,\text{aq}}^\square$ value is also in reasonable agreement with the corresponding experimental estimate. The calculated and experimental $k_{T,\text{aq}}^\square$ values both have a negative sign, but the magnitude of the experimental number is about twice as large, which may also result at least in part from an overstructuring of the solvation shells. In contrast, the calculated and experimental ion-pair $a_{p,\text{aq}}^\square$ values agree very well. Here also, however, the partitioning in terms of single-ion volume-expansivities differs significantly from that suggested by the recommended value $a_{p,\text{aq}}^\square[\text{H}^+] = -3.0 \times 10^{-8} \text{ m}^3 \text{ mol}^{-1} \text{ K}^{-1}$.

Finally, on the basis of the single-ion parameters obtained from the calculations, it is possible to suggest alternative values for the corresponding proton parameters, possibly differing from the recommended ones. Clearly, these suggested alternatives will only be similar for Na^+ and Cl^- , and thus acceptable, in cases where the ion-pair parameters are compatible with the corresponding experimental numbers. Expectedly, for the hydration free energy, the two alternative proton values are similar to each other and to the recommended value $\Delta G_{\text{hyd}}^\square = -1107.95 \text{ kJ mol}^{-1}$. For $\Delta H_{\text{hyd}}^\square$, s_{aq}^\square , and $k_{T,\text{aq}}^\square$, the estimates for the two ions are very different, and thus unreliable. For v_{aq}^\square , the two values are very close, and an estimate of about $-26.5 \times 10^{-6} \text{ m}^3 \text{ mol}^{-1}$ can be formulated for $v_{\text{aq}}^\square[\text{H}^+]$ on the basis of the simulations, as an alternative to the recommended value of $-4.5 \times 10^{-6} \text{ m}^3 \text{ mol}^{-1}$. For $c_{p,\text{aq}}^\square$, the two values are acceptably close given the large uncertainty on the calculated numbers, and an estimate of about $-366 \text{ J K}^{-1} \text{ mol}^{-1}$ can be formulated for $c_{p,\text{aq}}^\square[\text{H}^+]$ on the basis of the simulations, as an alternative to the recommended (but highly uncertain) value of $-86 \text{ J mol}^{-1} \text{ K}^{-1}$. For $a_{p,\text{aq}}^\square$, the two values are very close, and an estimate of about $+20.0 \times 10^{-8} \text{ m}^3 \text{ mol}^{-1} \text{ K}^{-1}$ can be formulated for $a_{p,\text{aq}}^\square[\text{H}^+]$ on the basis of the simulations, as an alternative to the recommended value of $-3.0 \times 10^{-8} \text{ m}^3 \text{ mol}^{-1} \text{ K}^{-1}$.

5. CONCLUSION

The aim of the present study was to investigate the feasibility of calculating and correcting derivative thermodynamic hydration and aqueous partial molar properties for Na^+ and Cl^- at P° and T° . As stated in section 1, this type of calculation is notoriously difficult, and the goal of this work was to cut a first path through an unexplored jungle rather than to reach quantitative agreement with sometimes rather uncertain experimental data. The results corresponding to different calculation schemes (methods I or II in conjunction with variants A or B) as well as the final results presented in Table 8 clearly show that, except for the hydration free energy itself, accurate methodological independence and quantitative agreement with even the most reliable experimental parameters (ion-pair properties) are not reached.

Expectedly, the calculated solvation free energies agree well with experimental ion-pair data and recommended single-ion values, due to appropriate calibration of the selected ion–solvent Lennard-Jones interaction parameters.¹⁰ However, the calculated ion-pair solvation enthalpies and partial molar entropies are too negative. This is probably due at least in part to the use of an implicit-polarization model for the ion–solvent interactions, resulting in an overstructuring of the hydration shells.^{65–67} The calculated partial molar heat capacities are affected by very large statistical uncertainties, and much longer ($\gg 60 \text{ ns}$) simulations would be required to achieve proper convergence. Given these uncertainties, the ion-pair results for this property are in acceptable agreement with experimental data. However, the single-ion results suggest a partitioning compatible with $c_{p,\text{aq}}^\square[\text{H}^+] = -366 \text{ J mol}^{-1} \text{ K}^{-1}$ for the proton, rather than with the recommended¹¹ (but highly uncertain) value of $-86 \text{ J mol}^{-1} \text{ K}^{-1}$. In particular, the former choice leads to a large and positive partial molar heat capacity for Cl^- , while the latter choice suggests a negative value instead. The calculated ion-pair partial molar volumes agree well with experimental ion-pair data, as is the case for the other alkali-halide ion pairs.¹⁰ However, here also, the single-ion results suggest a partitioning compatible with $v_{\text{aq}}^\square[\text{H}^+] = -26.5 \times 10^{-6} \text{ m}^3 \text{ mol}^{-1}$ for the proton, rather than with the recommended¹¹ value of $-4.5 \times 10^{-6} \text{ m}^3 \text{ mol}^{-1}$. The calculated ion-pair partial molar volume-expansivities agree well with experimental ion-pair data. However, here again, the single-ion results suggest a partitioning compatible with $a_{p,\text{aq}}^\square[\text{H}^+] = +20.0 \times 10^{-8} \text{ m}^3 \text{ mol}^{-1} \text{ K}^{-1}$ for the proton, rather than with the recommended¹¹ value of $-3.0 \times 10^{-8} \text{ m}^3 \text{ mol}^{-1} \text{ K}^{-1}$. In particular, the former choice leads to a large and negative partial molar volume-expansivity for Cl^- , while the latter choice suggests a small positive value instead. Finally, the calculated partial molar volume-compressibilities are affected by a strong sensitivity to the calculation protocol, and even the estimates considered most reliable in this work are not in good agreement with experimental ion-pair data. It should be kept in mind, however, that the experimental ion-pair data for the second-derivative quantities c_p^\square , k_T^\square , and a_p^\square rely on a handful of indirect and often relatively ancient determinations.¹¹ The uncertainty on the corresponding recommended proton values is even higher, considering that the tentative experimental determinations of these parameters are sparser, depend on specific extra-thermodynamic assumptions, and often present a limited consistency among each other. For these second-derivative parameters, it is thus not entirely clear whether these recommended values or the results of the present calculations

are to be considered most trustworthy. Finally, it should be kept in mind that the ion-pair data quoted here as experimental, as well as the proton data quoted here as recommended, are affected by an ambiguity related to the solute standard-state variant associated with the experimental numbers (section 2.2). On the basis of the most common types of experimental determinations,¹¹ a specific variant (standard or density-corrected) has been assumed here for each type of quantity, but an incorrect choice may lead to non-negligible errors, especially for the partial molar volume, heat capacity, and volume-compressibility (see $\Delta y_{\text{aq}}^{\ominus* \rightarrow \ominus}$ and $\Delta \Delta y_{\text{hyd}}^{\ominus* \rightarrow \ominus}$ values in Table 1).

Even if methodological independence and quantitative agreement with available experimental data is not yet reached, the present study underlines two important points: (i) the need to consider standard-state issues very carefully and (ii) the requirement to correct the calculated raw numbers appropriately. With respect to the latter point, the type-B correction term for finite-size effects and the type-C₁ correction term for improper potential summation are typically important, and their omission would lead to extremely large errors for all the calculated parameters. In this sense, the main merit of the present study is to set a clear framework for these types of calculations and to point toward directions for future improvements, with the ultimate goal of reaching a consistent and quantitative description of single-ion hydration thermodynamics in molecular dynamics simulations.

The residual dependence of the estimated parameters on the simulation protocol and calculation scheme results from three main problems: too short sampling times, too large finite-difference intervals, and inaccurate correction-scheme parameters. While the first two problems can in principle be remedied by investing more computing resources, a significant improvement in the correction scheme could be achieved by an explicit determination of the pressure and temperature dependences of the density and dielectric permittivity of the water model employed in the simulations. At present, the main reason for the discrepancies between the different calculation schemes (methods I or II in conjunction with variants A or B) probably results from using the approximation of eqs 47 and 48 for these functions. Three other lines of further methodological developments could involve: (i) the use of generalized-ensemble techniques^{69–73} for the direct sampling of system configurations over a finite pressure–temperature range within a single simulation, as an alternative to the multiple-point approach employed here; (ii) the use of appropriate fluctuation formulas^{57,74–85} for the direct evaluation of the pressure and temperature derivatives of the quantities considered, as another alternative to the multiple-point approach; or (iii) the use of multiple-parameter fitting formulas such as eqs 49 and 50, as an alternative to the finite-difference or least-squares fitting approach employed here. The application of these alternative schemes would render the calculation procedure more automatic, i.e., considerably reduce the human time involved in the (tedious) setup and postprocessing of the simulations. Note that the use of fluctuation formulas rests on the ability of the simulation procedure to accurately reproduce not only ensemble averages but also fluctuations appropriate for the isobaric–isothermal ensemble. For example, the Berendsen barostat and thermostat employed here⁴⁵ do not fulfill this condition, even in principle.^{80,86–88} Other formally isobaric–isothermal algorithms, e.g., the Andersen barostat⁸⁹ and the Nosé–Hoover thermostat,⁹⁰ may also fail to satisfy this

criterion in practice, due to numerical noise and ergodicity violations^{91–95} (steady-state rather than equilibrium situation). This issue introduces another factor of uncertainty in the simulation results, reason for which this approach was not considered in the present study. The comparison of finite-difference, generalized-ensemble and fluctuation approaches will be the scope of future work.

Provided that the residual methodological dependence of the estimated parameters can be reduced to an acceptable level, the remaining sources of discrepancies between calculation and experiment will reside in the inaccuracy of the molecular model employed and that of the experimental data to compare with. For the hydration enthalpy and the partial molar entropy, the experimental ion-pair parameters and, to a slightly lesser extent, the recommended single-ion parameters can probably be trusted. As mentioned above, the too negative values of the calculated ion-pair hydration enthalpies and aqueous partial molar entropies are probably due at least in part to the use of an implicit-polarization model for the ion–solvent interactions. The application of explicitly polarizable models^{65,66} or even of quantum-mechanical models (e.g., Car–Parrinello^{68,96–99} or quantum-mechanics molecular mechanics^{100–102}) would probably enable a more accurate representation of the enthalpy–entropy partitioning. Note in this respect that the present work considers relatively large monovalent ions, for which the electronic polarization of the solvent and the partially covalent character of ion–solvent interactions are expected to have limited effects. However, an appropriate treatment of these effects will become essential when small or/and polyvalent ions are considered. For the second-order derivatives, where the uncertainty in experimental ion-pair data and, to an even higher extent, recommended proton values is very large, it is not impossible that more accurate calculations with an improved molecular model ultimately provide results that are more trustworthy than experimentally inferred ones.

Finally, another important aspect of this research remains to be mentioned. If the calculation of derivative thermodynamic hydration and aqueous partial molar properties is highly relevant in the context of force-field parametrization and validation, it is also of interest *per se* in terms of the characterization of ionic hydration properties. For example, the recommended values as well as the results of the present calculations suggest that Na⁺ promotes the orientational polarization (enthalpy), the orientational correlation (entropy), and the contraction (volume) of the surrounding solvent, along with a decrease of the energetic thermal response (heat capacity), volumic pressure response (volume-compressibility), and volumic temperature response (volume-expansivity). While the first three effects are well-known, understanding the nature of the latter four in terms of a corresponding structural alteration of the hydrogen-bonding network of water by the ion remains challenging, and of great theoretical interest.

■ ASSOCIATED CONTENT

● Supporting Information

Details regarding the functional dependence of density and permittivity on pressure and temperature are provided, as well as additional calculation details for methods I and II. This information is available free of charge via the Internet at <http://pubs.acs.org>.

AUTHOR INFORMATION

Corresponding Author

*Tel.: +41 44 633 43 20. Fax: +41 44 632 10 39. E-mail: haniels@igc.phys.chem.ethz.ch.

Notes

The authors declare no competing financial interest.

ACKNOWLEDGMENTS

Financial support from the Swiss National Science Foundation (grant nos. 200021-132739 and 200021-138020) is gratefully acknowledged.

DEDICATION

This article is dedicated to Wilfred van Gunsteren in honor of his 65th birthday. Thanks, Wilfred, for your generosity, support, and enthusiasm over all the years. Your everlasting curiosity toward the fundamental problems of physical chemistry has been, and still is, a continuous source of inspiration for the four of us.

REFERENCES

- (1) Kastenholz, M. A.; Hünenberger, P. H. *J. Phys. Chem. B* **2004**, *108*, 774–788.
- (2) Reif, M. M.; Kräutler, V.; Kastenholz, M. A.; Daura, X.; Hünenberger, P. H. *J. Phys. Chem. B* **2009**, *113*, 3112–3128.
- (3) Warshel, A. *J. Phys. Chem.* **1982**, *86*, 2218–2224.
- (4) Lybrand, T. P.; Ghosh, I.; McCammon, J. A. *J. Am. Chem. Soc.* **1985**, *107*, 7793–7794.
- (5) Warshel, A.; Sussman, F.; King, G. *Biochemistry* **1986**, *25*, 8368–8372.
- (6) Straatsma, T. P.; Berendsen, H. J. C. *J. Chem. Phys.* **1988**, *89*, 5876–5886.
- (7) Kastenholz, M. A.; Hünenberger, P. H. *J. Chem. Phys.* **2006**, *124*, 124106/1–124106/27.
- (8) Kastenholz, M. A.; Hünenberger, P. H. *J. Chem. Phys.* **2006**, *124*, 224501/1–224501/20.
- (9) Reif, M. M.; Hünenberger, P. H. *J. Chem. Phys.* **2011**, *134*, 144103/1–144103/30.
- (10) Reif, M. M.; Hünenberger, P. H. *J. Chem. Phys.* **2011**, *134*, 144104/1–144104/25.
- (11) Hünenberger, P. H.; Reif, M. M. *Single-Ion Solvation: Experimental and Theoretical Approaches to Elusive Thermodynamic Quantities*, 1st ed.; Royal Society of Chemistry: London, U.K., 2011; Theoretical and Computational Chemistry Series, ISBN: 978-1-84755-187-0.
- (12) Berendsen, H. J. C.; Postma, J. P. M.; van Gunsteren, W. F.; Hermans, J. Interaction models for water in relation to protein hydration. In *Intermolecular Forces*; Pullman, B., Ed.; Reidel: Dordrecht, The Netherlands, 1981; pp 331–342.
- (13) Berendsen, H. J. C.; Grigera, J. R.; Straatsma, T. P. *J. Phys. Chem.* **1987**, *91*, 6269–6271.
- (14) Oostenbrink, C.; Villa, A.; Mark, A. E.; van Gunsteren, W. F. *J. Comput. Chem.* **2004**, *25*, 1656–1676.
- (15) Horta, B. A. C.; Fuchs, P. F. J.; van Gunsteren, W. F.; Hünenberger, P. H. *J. Chem. Theory Comput.* **2011**, *7*, 1016–1031.
- (16) Lynden-Bell, R. M.; Rasaiah, J. C. *J. Chem. Phys.* **1997**, *107*, 1981–1991.
- (17) Horinek, D.; Mamatkulov, S. I.; Netz, R. R. *J. Chem. Phys.* **2009**, *130*, 124507/1–124507/21.
- (18) Carlsson, J.; Åqvist, J. *J. Phys. Chem. B* **2009**, *113*, 10255–10260.
- (19) Reif, M. M. *Single-Ion Solvation Properties Using Atomistic Simulation*; ETH Thesis 18813, Zürich, Switzerland, DOI: 10.3929/ethz-a-006159535, 2010.
- (20) Irudayam, S. J.; Henchman, R. H. *Mol. Phys.* **2011**, *109*, 37–48.
- (21) Beck, T. L. *J. Phys. Chem. B* **2011**, *115*, 9776–9781.
- (22) Klasczyk, B.; Knecht, V. *J. Chem. Phys.* **2010**, *132*, 024109/1–024109/12.
- (23) Weerasinghe, S.; Smith, P. E. *J. Chem. Phys.* **2003**, *119*, 11342–11349.
- (24) Gee, M. B.; Cox, N. R.; Jiao, Y.; Benteinitis, N.; Weerasinghe, S.; Smith, P. E. *J. Chem. Theory Comput.* **2011**, *7*, 1369–1380.
- (25) Tetrode, H. *Ann. Phys.* **1912**, *344*, 255–256.
- (26) Tetrode, H. *Ann. Phys.* **1912**, *343*, 434–442.
- (27) Sackur, O. *Ann. Phys.* **1913**, *345*, 67–86.
- (28) Bartmess, J. E. *J. Phys. Chem.* **1994**, *98*, 6420–6424.
- (29) Latimer, W. M.; Kasper, C. *J. Am. Chem. Soc.* **1929**, *51*, 2293–2299.
- (30) Latimer, W. M. *Chem. Rev.* **1936**, *18*, 349–358.
- (31) Latimer, W. M.; Pitzer, K. S.; Slansky, C. M. *J. Chem. Phys.* **1939**, *7*, 108–111.
- (32) Marcus, Y. *J. Chem. Soc., Faraday Trans.* **1991**, *87*, 2995–2999.
- (33) Schmid, R.; Miah, A. M.; Sapunov, V. N. *Phys. Chem. Chem. Phys.* **2000**, *2*, 97–102.
- (34) Kelly, C. P.; Cramer, C. J.; Truhlar, D. G. *J. Phys. Chem. B* **2006**, *110*, 16066–16081.
- (35) Ben-Naim, A. *J. Solution Chem.* **2001**, *5*, 475–487.
- (36) Ben-Naim, A. *Molecular Theory of Solutions*; Oxford University Press: Oxford, U. K., 2006.
- (37) Hünenberger, P. H. Lattice-sum methods for computing electrostatic interactions in molecular simulations. In *Simulation and Theory of Electrostatic Interactions in Solution: Computational Chemistry, Biophysics, and Aqueous Solution*; Hummer, G., Pratt, L. R., Eds.; American Institute of Physics: New York, 1999; pp 17–83.
- (38) van Gunsteren, W. F.; Billeter, S. R.; Eising, A. A.; Hünenberger, P. H.; Krüger, P.; Mark, A. E.; Scott, W. R. P.; Tironi, I. G. *Biomolecular simulation: The GROMOS96 manual and user guide*; Verlag der Fachvereine: Zürich, Switzerland, 1996.
- (39) Scott, W. R. P.; Hünenberger, P. H.; Tironi, I. G.; Mark, A. E.; Billeter, S. R.; Fennel, J.; Torda, A. E.; Huber, T.; Krüger, P.; van Gunsteren, W. F. *J. Phys. Chem. A* **1999**, *103*, 3596–3607.
- (40) Hockney, R. W.; Eastwood, J. W. *Computer Simulation Using Particles*; McGraw-Hill, New York, 1981.
- (41) Christen, M.; Hünenberger, P. H.; Bakowies, D.; Baron, R.; Bürgi, R.; Geerke, D. P.; Heinz, T. N.; Kastenholz, M. A.; Kräutler, V.; Oostenbrink, C.; Peter, C.; Trzesniak, D.; van Gunsteren, W. F. *J. Comput. Chem.* **2005**, *26*, 1719–1751.
- (42) Barker, J. A.; Watts, R. O. *Mol. Phys.* **1973**, *26*, 789–792.
- (43) Hockney, R. W. *Methods Comput. Phys.* **1970**, *9*, 136–211.
- (44) Ryckaert, J.-P.; Ciccotti, G.; Berendsen, H. J. C. *J. Comput. Phys.* **1977**, *23*, 327–341.
- (45) Berendsen, H. J. C.; Postma, J. P. M.; van Gunsteren, W. F.; di Nola, A.; Haak, J. R. *J. Chem. Phys.* **1984**, *81*, 3684–3690.
- (46) Kell, G. S. *J. Chem. Eng. Data* **1967**, *12*, 66–69.
- (47) Luty, B. A.; Tironi, I. G.; van Gunsteren, W. F. *J. Chem. Phys.* **1995**, *103*, 3014–3021.
- (48) Hünenberger, P. H. *J. Chem. Phys.* **2000**, *113*, 10464–10476.
- (49) Deserno, M.; Holm, C. *J. Chem. Phys.* **1998**, *109*, 7678–7693.
- (50) Deserno, M.; Holm, C. *J. Chem. Phys.* **1998**, *109*, 7694–7701.
- (51) Redlack, A.; Grindlay, J. *Can. J. Phys.* **1972**, *50*, 2815–2825.
- (52) Nijboer, B. R. A.; Ruijgrok, T. W. *J. Stat. Phys.* **1988**, *53*, 361–382.
- (53) Hummer, G.; Pratt, L. R.; Garcia, A. E. *J. Phys. Chem.* **1996**, *100*, 1206–1215.
- (54) Heinz, T. N.; Hünenberger, P. H. *J. Chem. Phys.* **2005**, *123*, 034107/1–034107/19.
- (55) Bogusz, S.; Cheatham, T. E.; Brooks, B. R. *J. Chem. Phys.* **1998**, *108*, 7070–7084.
- (56) Glättli, A.; Daura, X.; van Gunsteren, W. F. *J. Chem. Phys.* **2002**, *116*, 9811–9828.
- (57) Allen, M. P.; Tildesley, D. J. *Computer Simulation of Liquids*; Oxford University Press: New York, 1987.
- (58) Bevington, P. R.; Robinson, D. K. *Data Reduction and Error Analysis for the Physical Sciences*, 3rd ed.; McGraw-Hill: New York, 2003; ISBN: 0-07-247227-8.

- (59) Kirkwood, J. G. *J. Chem. Phys.* **1935**, *3*, 300–313.
- (60) Born, M. *Z. Phys.* **1920**, *1*, 45–48.
- (61) Bradley, D. J.; Pitzer, K. S. *J. Phys. Chem.* **1979**, *83*, 1599–1603.
- (62) Fornberg, B. *Math. Comput.* **1988**, *51*, 699–706.
- (63) Wagner, W.; Pruss, A. *J. Phys. Chem. Ref. Data* **2002**, *31*, 387–535.
- (64) Pashikanti, K. Implementation of IAPWS-95 specification for water and steam properties, Version 2.0, 2010/6/26. Available from <http://code.google.com/p/proph2o> (accessed July 4, 2011).
- (65) Stuart, S. J.; Berne, B. J. *J. Phys. Chem.* **1996**, *100*, 11934–11943.
- (66) Grossfield, A.; Ren, P.; Ponder, J. W. *J. Am. Chem. Soc.* **2003**, *125*, 15671–15682.
- (67) Trumm, M.; Martínez, Y. O. G.; Réal, F.; Masella, M.; Vallet, V.; Schimmelpfennig, B. *J. Chem. Phys.* **2012**, *136*, 044509/1–044509/11.
- (68) Whitfield, T. W.; Varma, S.; Harder, E.; Lamoureux, G.; Rempe, S. B.; Roux, B. *J. Chem. Theory Comput.* **2007**, *3*, 2068–2082.
- (69) Andrade, J. S.; Almeida, M. P.; Moreira, A. A.; Farias, G. A. *Phys. Rev. E* **2002**, *65*, 036121/1–036121/5.
- (70) Barth, E. J.; Laird, B. B.; Leimkuhler, B. J. *J. Chem. Phys.* **2003**, *118*, 5759–5768.
- (71) Minary, P.; Martyna, G. J.; Tuckerman, M. E. *J. Chem. Phys.* **2003**, *118*, 2510–2526.
- (72) Okamoto, Y. *J. Mol. Graphics Modell.* **2004**, *22*, 425–439.
- (73) Itoh, S. G.; Okumura, H.; Okamoto, Y. *Mol. Simul.* **2007**, *33*, 47–56.
- (74) Lebowitz, J. L.; Percus, J. K.; Verlet, L. *Phys. Rev.* **1967**, *153*, 250–254.
- (75) Ray, J. R.; Graben, H. W. *Mol. Phys.* **1981**, *43*, 1293–1297.
- (76) Ray, J. R. *Am. J. Phys.* **1982**, *50*, 1035–1038.
- (77) Kratky, K. W. *Phys. Rev. A* **1985**, *31*, 945–950.
- (78) Debenedetti, P. G. *J. Chem. Phys.* **1987**, *86*, 7126–7137.
- (79) Debenedetti, P. G. *J. Chem. Phys.* **1988**, *88*, 2681–2684.
- (80) Morishita, T. *J. Chem. Phys.* **2000**, *113*, 2976–2982.
- (81) Lagache, M.; Ungerer, P.; Boutin, A.; Fuchs, A. H. *Phys. Chem. Chem. Phys.* **2010**, *3*, 4333–4339.
- (82) D'Alessandro, M.; Tenenbaum, A.; Amadei, A. *J. Phys. Chem. B* **2002**, *106*, 5050–5057.
- (83) Meier, K.; Kabelac, S. *J. Chem. Phys.* **2006**, *124*, 054104/1–064104/10.
- (84) Schnell, S. K.; Liu, X.; Simon, J.-M.; Bardow, A.; Bedeaux, D.; Vlugt, T. J. H.; Kjelstrup, S. *J. Phys. Chem. B* **2011**, *115*, 10911–10918.
- (85) Colangeli, M.; Rondoni, L. *Physica D* **2012**, *241*, 681–691.
- (86) Mudi, A.; Chakravarty, C. *Mol. Phys.* **2004**, *102*, 681–685.
- (87) Mor, A.; Ziv, G.; Levy, Y. *J. Comput. Chem.* **2008**, *29*, 1992–1998.
- (88) Rosta, E.; Buchete, N.-V.; Hummer, G. *J. Chem. Theory Comput.* **2009**, *5*, 1393–1399.
- (89) Andersen, H. C. *J. Chem. Phys.* **1980**, *72*, 2384–2393.
- (90) Hoover, W. G. *Phys. Rev. A* **1985**, *31*, 1695–1697.
- (91) Harvey, S. C.; Tan, R.K.-Z.; Cheatham, T. E., III. *J. Comput. Chem.* **1998**, *19*, 726–740.
- (92) Hünenberger, P. H. *Adv. Polym. Sci.* **2005**, *173*, 105–149.
- (93) Lingenheil, M.; Denschlag, R.; Reichold, R.; Tavan, P. *J. Chem. Theory Comput.* **2008**, *4*, 1293–1306.
- (94) Cooke, B.; Schmidler, S. C. *J. Chem. Phys.* **2008**, *129*, 164112/1–164112/17.
- (95) Eastwood, M. P.; Stafford, K. A.; Lippert, R. A.; Jensen, M. Ø.; Maragakis, P.; Predescu, C.; Dror, R. O.; Shaw, D. E. *J. Chem. Theory Comput.* **2010**, *6*, 2045–2058.
- (96) Guàrdia, E.; Skarmoutsos, I. *J. Chem. Theory Comput.* **2009**, *5*, 1449–1453.
- (97) Leung, K.; Rempe, S. B.; von Lilienfeld, O. A. *J. Chem. Phys.* **2009**, *130*, 204507/1–204507/11.
- (98) Chen, E. S.; Chen, E. C. M. *J. Chem. Phys.* **2010**, *133*, 047103/1–047103/2.
- (99) Rempe, S. B.; Leung, K. *J. Chem. Phys.* **2010**, *133*, 047104/1–047104/2.
- (100) Rode, B. M.; Schwenk, C. F.; Tongraar, A. *J. Mol. Liq.* **2004**, *110*, 105–122.
- (101) Schwenk, C. F.; Loeffler, H. H.; Rode, B. M. *J. Chem. Phys.* **2001**, *115*, 10808–10813.
- (102) Rowley, C. N.; Roux, B. *J. Chem. Theory Comput.* **2012**, DOI: 10.1021/ct300091w.
- (103) Kaye, G. W. C.; Laby, T. H. Tables of Physical, Chemical Constants. 3.1.2 Properties of the elements, Kaye and Laby Online, Version 1.0, 2005. Available from www.kayelaby.npl.co.uk (accessed August 1, 2009).